SOME STRUCTURAL INVESTIGATIONS IN HIGH-TEMPERATURE Y—Ba—Cu—O SUPERCONDUCTORS

By

Charagondla Narsimha rao

DEPARTMENT OF METALLURGICAL ENGINEERING

INDIAN INSTITUTE OF TECHNOLOGY KANPUR

DECEMBER, 1992

SOME STRUCTURAL INVESTIGATIONS IN HIGH-TEMPERATURE Y-Ba-Cu-O SUPERCONDUCTORS

A Thesis Submitted

In Partial Fulfilment of the Requirements

for the Degree of

MASTER OF TECHNOLOGY

by

CHARAGONDLA NARSIMHA RAO

to the

DEPARTMENT OF METALLURGICAL ENGINEERING

INDIAN INSTITUTE OF TECHNOLOGY KANPUR

December, 1992

CERTIFICATE

It is certified that the work contained in the thesis entitled *"Some Structural Investigations in High-Temperature Y-Ba-Cu-O Superconductors"*, has been carried out under my supervision and that this work has not been submitted elsewhere for a degree.

M. N. Shetty
~~Professor~~
Department of Metallurgical Engineering
Indian Institute of Technology
Kanpur

December, 1992

ACKNOWLEDGEMENTS

I wish to express my deep sense of indebtness and grati to **Dr. M. N. Shetty, Professor, Department of Metallurg Engineering, IIT Kanpur**, who proposed, guided and helped this to completion through his uncountable suggestions and construc criticisms.

I am grateful to Mr. S. V. Sharma, K. Srinivasan, Raj Aggarwal and many other friends for their immense help and company without their timely assistance the work would not completed in time. My sincere thanks to Mr. V. P. Gupta, Mr. N. Mungole, Mr. B. Sharma and Mr. Umashankar for their techn help in need.

Finally, but not perfunctorily, I wish to thank Mr. Yash for his diligence in preparing the typed manuscript at shortest notice of time.

Narsimha Rao Charagond

Dedicated to

My parents

Smt. Radha & Sri C.A. Rao

CONTENTS

SYNOPSIS

Grain orientation in High-T_c Y-Ba-Cu-O Ceramic superconducting system are produced by cold pressing and annealing process. Superconducting phase, $YBa_2Cu_3O_{7-\delta}$, is prepared from the powders of Y_2O_3, $BaCO_3$ and CuO through solid state reactions route. In order to produce preferred grain orientations, the samples are reannealed twice at 700°C/10 h in Oxygen atmosphere. At each stage, samples are characterized by SEM, and X-ray diffraction measurements. Effect of compaction pressure and effect of heating rate on sintered densities are studied.

X-ray diffraction peaks and SEM-EDAX studies have clearly shown the formation of superconducting phase while, X-band EPR measurements have confirmed the formation of this phase. Reannealed samples have shown that intensities of (001) peaks increased with concurrent decrease in (110) and 103) peaks. This corroborates that grain orientations occurred parallel to the pressure axis i.e., the C-axis is oriented parallel to the pressure axis with ab-plane perpendicular to the pressure direction. Sintered densities are found to increase with increase in compaction pressures and decrease in heating rates of samples.

LIST OF FIGURES

LIST OF TABLES

Symbol	Meaning
T_c	Critical Temperature
J_c	Critical Current Density
H_{c_1}, B_{c_1}	Lower Critical magnetic Field
H_{c_2}, B_{c_2}	Upper Critical Magnetic Field
M	Magnetisation
χ	Magnetic Susceptibility
H	Magnetic Field Strength
a,b,c	Lattice Parameters in an Unitcell
λ_L	London Penetration Depth
μ_o	Permeability of Freespace
123	$YBa_2Cu_3O_{7-x}$ Phase
211	$Y_2Ba_1Cu_1O_5$ Phase
231	$Y_2Ba_3Cu_1O_x$ Phase
T_c^{Onset}	Superconducting Onset Temperature
β,γ	Phases of $BaCO_3$
G	Gauss
T	Tesla
Hz	Hertz
Ω	Ohm

CHAPTER 1

INTRODUCTION:

The liquefaction of helium by Kamerlingh onnes in 1908 was the first mile stone which caused experimental studies on superconductivity. In 1911, Onnes discovered superconductivity in mercury (T_c=4.1K) at the university of Lieden in Holland. It was soon found that many other elements, alloys and intermetallic compounds become superconducting. Over the years, the highest transition temperature had been gradually increased from the 4.1K of Hg to 23K in the compound Nb_3Ge.

One of the most exciting developments in Science in recent times is the discovery of high-temperature superconducting oxides. There has been a flood of activity following the break through discovery of high-T_c perovskite-type superconductors by Bednorz and Müller [ref. 1] in La-Ba-Cu-O system. Chu et al, [ref. 2] claimed a 40 K onset temperature in La-Ba-Cu-O system under pressure and later Cava et al., [ref. 3] reported a 36.2 K superconducting transition temperature in La-Sr-Cu-O system. The subsequent discovery of even higher - T_c oxide in the system Y-Ba-Cu-O (T_c>90K) by Wu et al [ref. 4] has stimulated extensive investigation in the preparation and characterisation of high temperature ceramic superconductors. Cava et al [ref. 5] identified the superconducting phase in the Y-Ba-Cu-O system as $Y_1Ba_2Cu_3O_{7-\delta}$ with orthorhombic crystal structure having lattice parameters, a = 3.8218 A^o, b = 3.8913 A^o, and c = 11.677A^o. It was also determined that $YBa_2Cu_3O_{7-\delta}$ exists in tetragonal form, with a = 3.8533 A^o, C = 11.7631 A^o [ref. 6], depending upon the value of δ and this phase is a non-supercoducting phase. Hor et

al, [ref. 6], confirmed the superconductivity above 90 K in Y-Ba-Cu-O system both at ambient and high pressure.

While several new high - T_c materials were developed and the search for higher T_c materials continues most of the research activities focussed on the popular system Y-Ba-Cu-O because of the ease with which it can be prepared to obtain the single superconducting phase compared to the other systems. The new superconductors are ceramic oxides and have the mechanical properties of ceramics. They are very brittle, further, the conduction is highly anisotropic high current densities are obtained only when the flow is along two dimensional sheets of copper oxide. The sheets are separated by divalent and trivalent ions. High current densities are not found in the usual polycrystalline material in which the crystallites have random orientation.

Practical Superconductors Must essentially possess four useful properties: a high-superconducting transition temperature, T_c; a high upper critical magnetic field, B_{c_2}; a high critical current density, J_c; and fabricability into useful forms such as wires, ribbons, rods and films.

For most electrical applications, high J_c of more than 10^5 A/cm^2 is required [ref. 8]. Single crystals and thin films of YBCO were found to have $J_c \sim 10^6$ A/cm^2, while this value for bulk superconductors is very low. Since the growth of large single crystals is not only expensive but also time consuming, attention is now focused on the grain oriented bulk superconductors [ref. 9-12] polycrystalline YBCO materials with some degree of texture

have been produced by hot-pressing [ref. 9, 13, 16], pressforging [ref. 12, 14], melt method [ref. 15] and by a field-induced orientation method [ref. 11].

In the present work, grain oriented $Y_1Ba_2Cu_3O_{7-\delta}$ superconductors are produced by coldpressing and annealing and are characterized by various techniques.

1.1 Characteristic Properties of a Superconductor:

When metals are cooled to lower temperatures, some of them exhibit an abrupt drop in resistivity and enter a state in which there is no resistance to the flow of current called "superconducting state". The temperature at which the transition to the superconducting state occurs is designated as T_c.

Meissner Effect:

One of the properties that makes a superconductor different from a perfect conductor is the Meissner Effect which was discovered by Meissner and Ochsenfeld in 1933. This effect states that upon cooling a magnetic field is expelled from a normal metal specimen when it passes through T_c and becomes a superconductor. The exclusion of magnetic lines of flux from an object in the superconducting state is shown schematically in Fig. 1.1 where a penetration depth, designated as λ_L, is indicated. Typical values of λ_L are of the order of 50 nm.

In superconducting state,

$$B = \mu_o H + \mu_o M = 0$$

So, the susceptibility χ is

$$\chi = \frac{M}{H} = -1$$

where H is the applied magnetic field and M is magnetization. The superconductor therefore acts as an ideal diamagnet.

If the superconductor is subjected to a sufficiently strong magnetic field, it is observed that the supercoductivity is destroyed. The field at which it is destroyed is called the critical field, H_c. This field is a function of temperature and obeys the following parabolic law.

$$\frac{H_c(T)}{H_c(0)} = 1 - \left(\frac{T}{T_c}\right)^2$$

where $H_c(T)$ and $H_c(0)$ are the critical fields at temperature T and 0 respectively.

1.2 Type I and Type II Superconductors:

Depending upon the variation of magnetisation with applied magnetic field superconductors have been classified into two types. Type I or the ideal superconductor when placed in a magnetic field repels the flux lines completely, till the magnetic field attains the critical value H_c. The magnetization M is equal to -H up to H_c, where it suddenly drops to zero, as shown in Fig. 1.2. Type II or hard superconductors are those in which the ideal behaviour is seen upto a lower critical field H_{c_1}, beyond which the magnetization gradually changes and attains zero at an uppercritical field designated H_{c_2}, Fig. 1.3. The Meissner effect is incomplete in the region between H_{c_1} and H_{c_2}; this region is known as the vortex region. The magnetic flux lines gradually penetrate the solid, as the field is increased beyond H_{c_1} and the penetration is complete only at H_{c_2}.

1.3 Oxide Superconductors:

Although the phenomenon of superconductivity has been known since 1911, oxide superconductors only came on the scene about 25

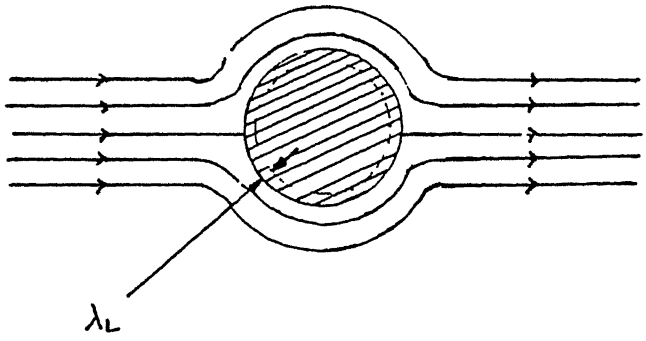

FIG. 1.1 AN OBJECT IN THE SUPERCONDUCTING STATE IN A MAGNETIC FIELD, λ_L IS PENETRATION DEPTH [REF. 44]

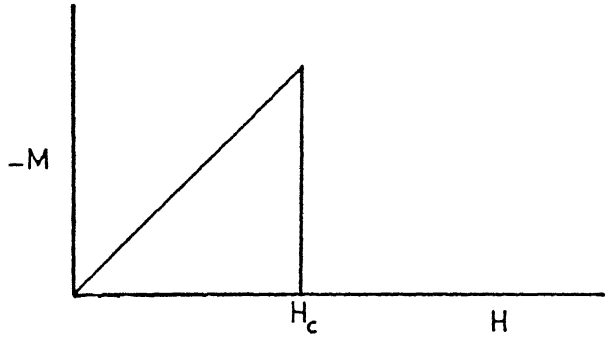

FIG. 1.2 MAGNETIZATION CURVES OF TYPE I SUPERCONDUCTORS [REF. 45]

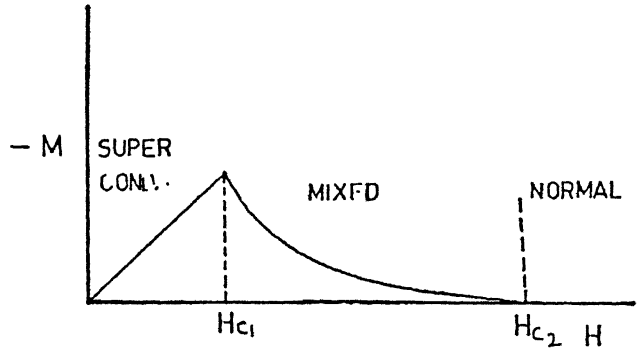

FIG. 1.3 MAGNETIZATION CURVES OF TYPE II SUPERCONDUCTORS [REF. 45]

years ago (Table 1.1). Initially oxide superconductors did not cause much excitement because their T_c's were lower than those found for intermetallic compounds. However, some oxide superconductors makeup a remarkable class of superconductors, holding records for highest T_c and highest critical field by wide margins [ref. 44]. All the oxide superconductors are type II superconductors.

While the search for new high T_c materials continues the system Y-Ba-Cu-O is of critical importance because of its potential feasibility as a high temperature superconductor.

Table 1.1 : Oxide Superconductors

Oxide	T_c (K)	Date reported	Reference
$SrTiO_3$	0.7	1964	27
Ag_7O_8X	1.0	1966	27
NbO	1.0	1965	27
TiO	2.0	1965	27
A_xMoO_3	4.0	1966	27
$A_xR_eO_3$	4.0	1969	27
A_xWO_3	6.0	1965	27
$LiTi_2O_4$	13.0	1974	27
$Ba(Pb,Bi)O_3$	13.0	1975	27
$(La,A)_2Cu_2O_4$	40.0	1986	1-3
$Bi_4Ca_3Sr_3Cu_4O_{16}$	85.0	1988	39
$RBa_2Cu_3O_7$	95.0	1987	4
$Bi_2Ca_2Sr_2Cu_3O_{7-\delta}$	110.0	1988	39
$Tl_2Ca_2Ba_2Cu_3O_{10}$	125.0	1988	39
$YBa_2Cu_3F_xO_y$	155.0	1987	39

R = Lanthanide Rare-Earth ion, A = Alkaline or Alkaline-Earth ion
X = NO_3^-, HF_2^-. ClO_4^-, BF_4^-

1.3.1 Phase Equilibria of Y-Ba-Cu-O System:

The synthesis of oxide superconductors is usually made out of ceramics and the possible large scale applications of these superconductors might take place after improving the ceramic preparation methods. As a consequence, the knowledge of the superconducting phase diagram is essential, to be able to differentiate properties related to the intrinsic behaviour of the material from those arising from the morphology of structural defects in the material [ref. 17]. Therefore, much of early chemical work in Y-Ba-Cu-O system was directed to this end. However, despite considerable efforts, understanding of the (sub) solidus and the liquid phase is somewhat tentative. One ternary phase diagram at 950°-1000° C with a number of phases is shown in Fig. 1.4. An alternative diagram at 950°C is shown in Fig. 1.5. As shown in Fig. 1.4 there are three pseudoternary compounds: the (123) super conducting phase $YBa_2Cu_3O_x$, the (211) semiconducting phase Y_2BaCuO_5 and the (132) problematic phase $YBa_3Cu_2O_x$.

The BaO-CuO binary compound is very complicated and is only shown in dashed lines in Fig. 1.5. The BaO-CuO binary compounds are hygroscopic and decompose to hydrates and carbonates during analysis. They also decompose above 850°C. However Frase et al [ref. 18] shows that $BaCuO_2$ decomposes just above 950°C. The central section of Fig. 1.5 shows tie lines radiating from the superconducting $Y_1Ba_2Cu_3O_x$ compound. The $Y_2Ba_1Cu_1O_x$ phase has tie lines to Y_2O_3, CuO, BaY_2O_4, $BaCuO_2$, $Y_2Cu_2O_5$ and a new phase $Y_1Ba_3Cu_2O_x$.

In the CuO-rich end of the diagram, all compositions which were deficient in Y_2O_3 from the $Y_1Ba_2Cu_3O_x$ composition showed

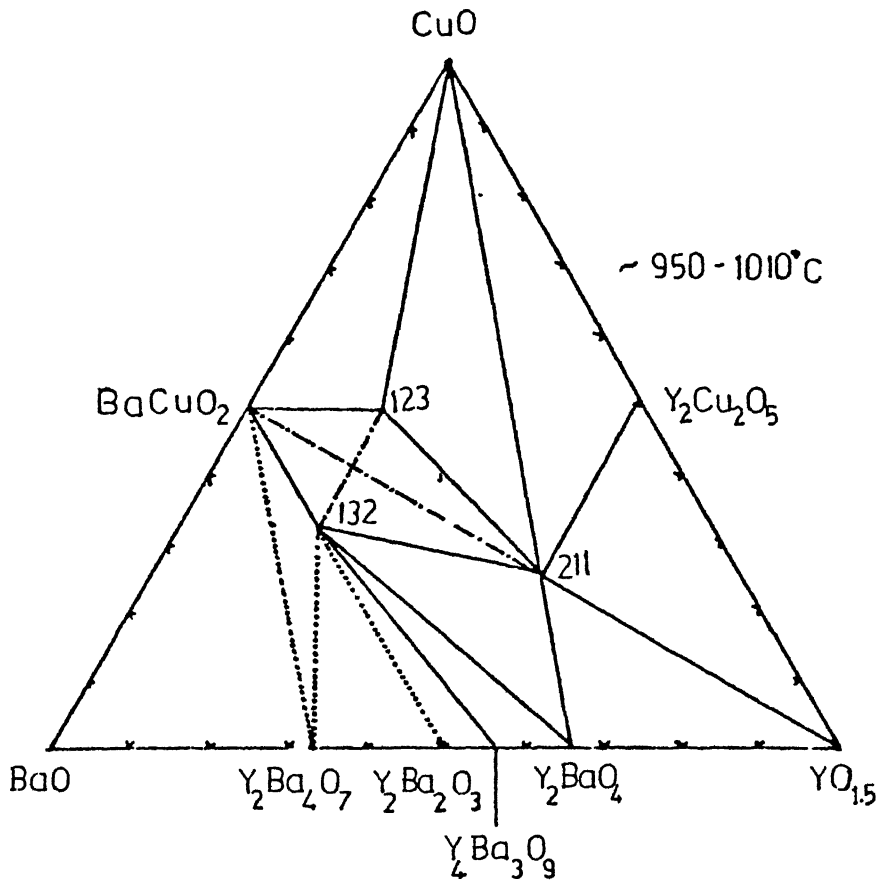

FIG. 1.4 TENTATIVE COMPATIBILITY RELATIONS IN THE SYSTEM $\frac{1}{2}Y_2O_3$ - BaO - CuO AT ~950°C

123 - $YBa_2Cu_3O_{7-x}$ 211 - Y_2BaCuO_5, 132 - $YBa_3Cu_2O_x$ [REF. 46]

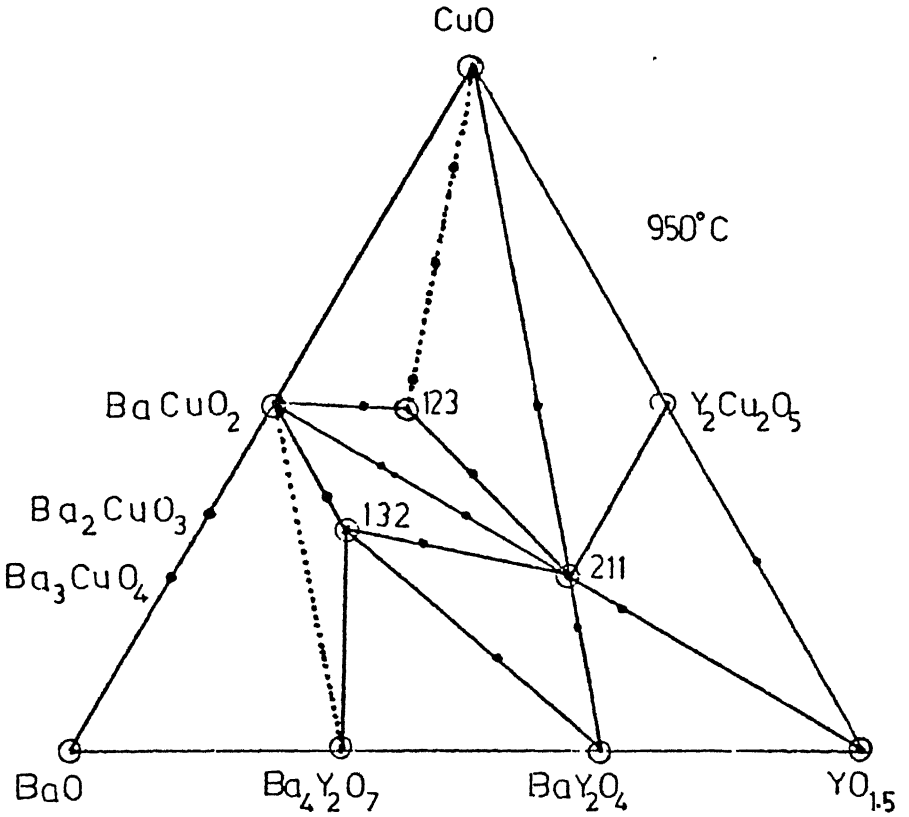

FIG. 1.5 COMPATIBILITY REGIONS IN THE PSEUDOTERNARY Y_2O_3-BaO-CuO AS DETERMINED AT 950°C
-123, 211, 132 REFER TO THE PHASE COMPOSITIONS $YBa_2Cu_3O_x$, Y_2BaCuO_5, $YBa_3Cu_2O_x$ RESPECTIVELY [REF. 18]

atleast some liquid formation at 950°C. Compositions along the tie line from $Y_1Ba_2Cu_3O_x$ to CuO showed no liquid at 880°C, but at 930°C liquid was formed. The presence of a compatible liquid phase suggests that it would be suitable for liquid phase sintering of superconducting phase. By contrast, compositions on tie line joining CuO to $Y_2Ba_1Cu_1O_x$ shows no signs of liquid formation after even heating at 950°C.

Hinks et al, [ref. 19] reported that only those samples in phase regions containing $Y_1Ba_2Cu_3O_{6.5}$ (Oxygen concentration inferred from charge balance) are superconducting near 90 K and superconductivity in samples residing outside these regions. This indicates that $YBa_2Cu_3O_{6.5}$ is the high - T_c superconducting compound in this system. It was demonstrated that $Y_1Ba_2Cu_3O_{6.5}$ exists as a single phase material by both neutron and x-ray diffraction patterns Fig. 1.6. Moving away from $Y_1Ba_2Cu_3O_{6.5}$ along the $(Y_{1-x}Ba_x)Cu$ composition line (50% Cu), in either direction from stoichiometric compound, new peaks appear in diffraction pattern. For $x < 0.67$ peaks attribute to Y_2BaCuO_5 and CuO appear, while for $x > 0.67$, only $BaCuO_2$ is observed. It was confirmed that $Y_1Ba_2Cu_3O_{6.5}$ compound is the superconducting phase by resistivity and critical current density measurements. Fig. 1.7(a) shows plot between onset temperature (T_c onset) of superconducting transition and the zero Cu composition line. T_c onset is almost constant with varying Ba concentration (x), showing that a single phase with well defined stoichiometry is responsible for superconductivity. Critical current density, which is sensitive to the volume fraction of super-conducting phase, measurements made at 77 K: composition versus critical

current density plot is shown in Fig. 1.7(b). It can be noted that T_c exhibits a maximum of (168 A/cm^2) at x = 0.67 ($Y_1Ba_2Cu_3O_{6.5}$), indicating that volume fraction of superconducting phase is maximum at this composition. Hinks et al, [ref. 19] also reports that samples with a higher barium content (x>0.67) have high porosity. This would account for the rapid decrease in J_c to very low values (< 2 A/cm^2) for x > 0.67 which in turn is in accordance with the reduction in T_c for samples as illustrated in Fig. 1.7(b).

From the above results it is clear that the (123) phase is virtually a point compound, exhibiting little or no solid solubility. This explains the difficulty many earlier researchers had in obtaining single phase materials.

Other processing difficulties arises from the large number of phase fields that the raw materials must cross in order to reach the (123) phase. This gives rise to the possibility of many side reactions during firing. It can also be seen that there are several phasetransitions that take place in the temperature range 900-1000^{o}C at which (123) phase is normally processed. These observations make it clear that very careful processing must be employed to achieve materials of optimal quality.

1.3.2 Crystal Structure of $YBa_2Cu_3O_{7-x}$:

It is essential to know about the crystal structure of a solid to understand its microscopic properties. Today the crystal structure of $YBa_2Cu_3O_{7-\delta}$ is completely known.

Ideal Perovskite Structure: The perovskite structure shown in Fig. 1.8, consists of three distinct elements with a chemical formula

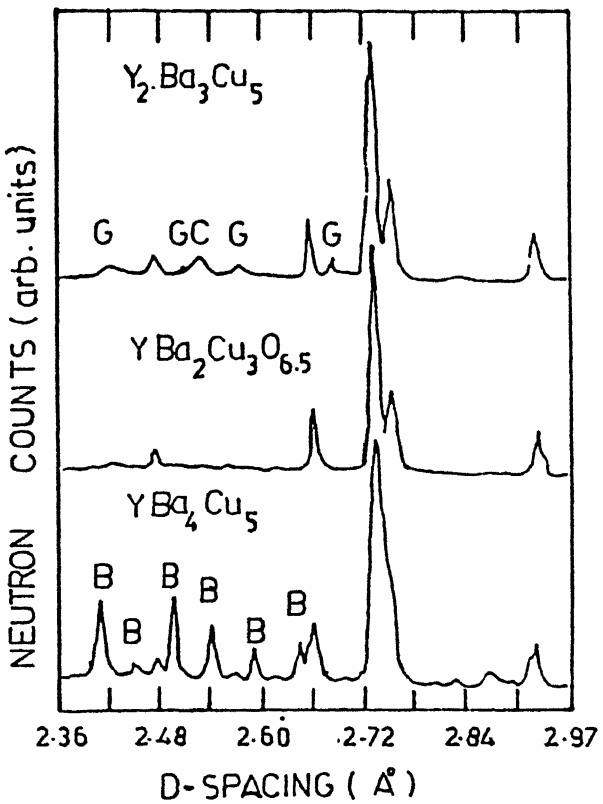

FIG. 1·6 NEUTRON DIFFRATION PATTERNS WHICH SHOW THE APPEARENCE OF SECOND PHASES AS THE STOICHIOMETRY MOVES AWAY FROM $YBa_2Cu_3O_{6.5}$. THE IMPURITY PHASES ARE IDENTIFIED AS B=$BaCuO_2$, G=Y_2BaCuO_5 , C=CuO (ref. 30)

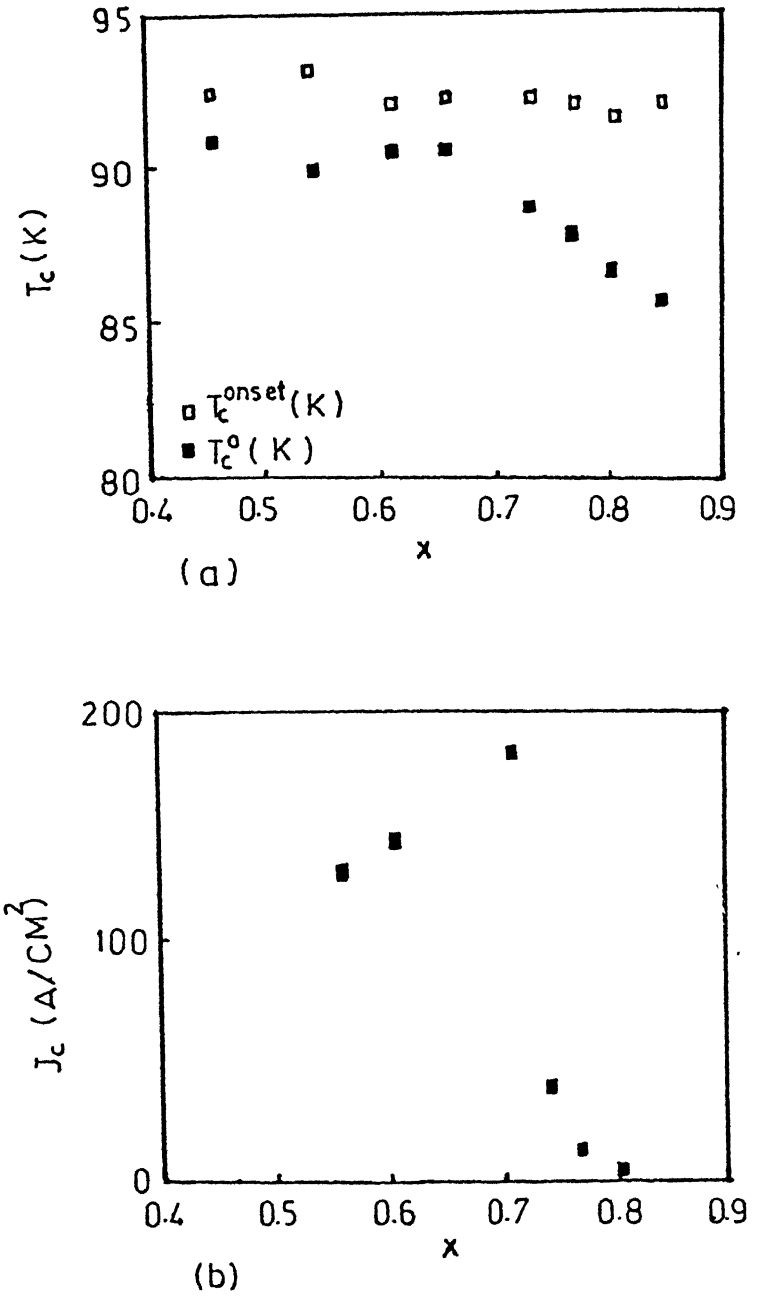

FIG. 1·7. (a) ONSET OF SUPERCONDUCTING TRANSITION TEMPERATURE (T_c^{onset}) & THE ZERO RESISTANCE TEMPERATURE (T_c^o) vs. INCREASING Ba COMPOSITION (x) ALONG THE ($Y_{1-x}Ba_x$)Cu COMPOSITION LINE; (b) CRITICAL CURRENT DENSITY AT 77K vs. INCREASING Ba COMPOSITION (x) (ref. 30)

AMO_3, where A cations occupy the centre of the cube, M cations occupy corners and oxygen anions occupy the centre of the edges of cube.

Crystal Structure of $YBa_2Cu_3O_{7-x}$: Fig. 1.9 shows the Y-Ba-Cu-O crystal structure shown by many neutron diffraction studies [ref. 20-22], and supported by many x-ray diffraction [ref. 21,23] and electron diffraction studies [ref. 24, 25]. The structure resembles that of Perovskite type and can be created by stacking three AMO_3 unit cells, removing an oxygen atom at $(0,0,\frac{1}{2})$ to make the composition $A_3M_3O_8$, removing an oxygen atom at $(\frac{1}{2},0,0)$ to make the composition $A_3M_3O_7$, and allowing relaxations. If the stoichiometry falls below O_7, then $(0,\frac{1}{2},0)$ sites becomes partially occupied. AT $O_{6.5}$ they are 50% full.

The superconducting phase is orthorhombic with a unit cell voluem = 173.30 A^{o^3} (a = 3.8185 A^o, b = 3.8856 A^o and c = 11.680 A^o). However, depending upon the x values, a reversible transformation occurs at $x \approx 6.5$ from orthorhombic symmetry to teragonal symmetry [ref. 26]. Table 1.2 and 1.3 shows the fractional atomic coordinates for $YBa_2Cu_3O_7$ and $YBa_2Cu_3O_6$ respectively. Oxygen valancies are localised in ordered way at $(00\frac{1}{2})$ (in the plane containing atom Y) and at $(\frac{1}{2}00)$ (in the plane containing Cu(I)), producing two crystallographically and chemically different Cu sites [ref. 27,28]. Cu(I) sites are surrounded by square planar oxygen coordination which are linked together in the b-c plane forming one-dimensional chains parallel to b-axis. Cu(2) is five fold coordinated in a square pyramid arrangement of oxygen atoms. The comparison of the bond distances

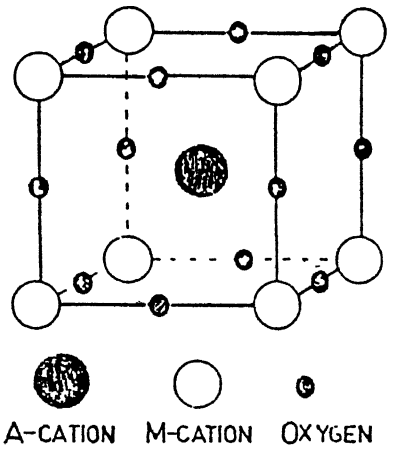

FIG. 1.8 IDEAL PEROVSKITE STRUCTURE [REF. 47]

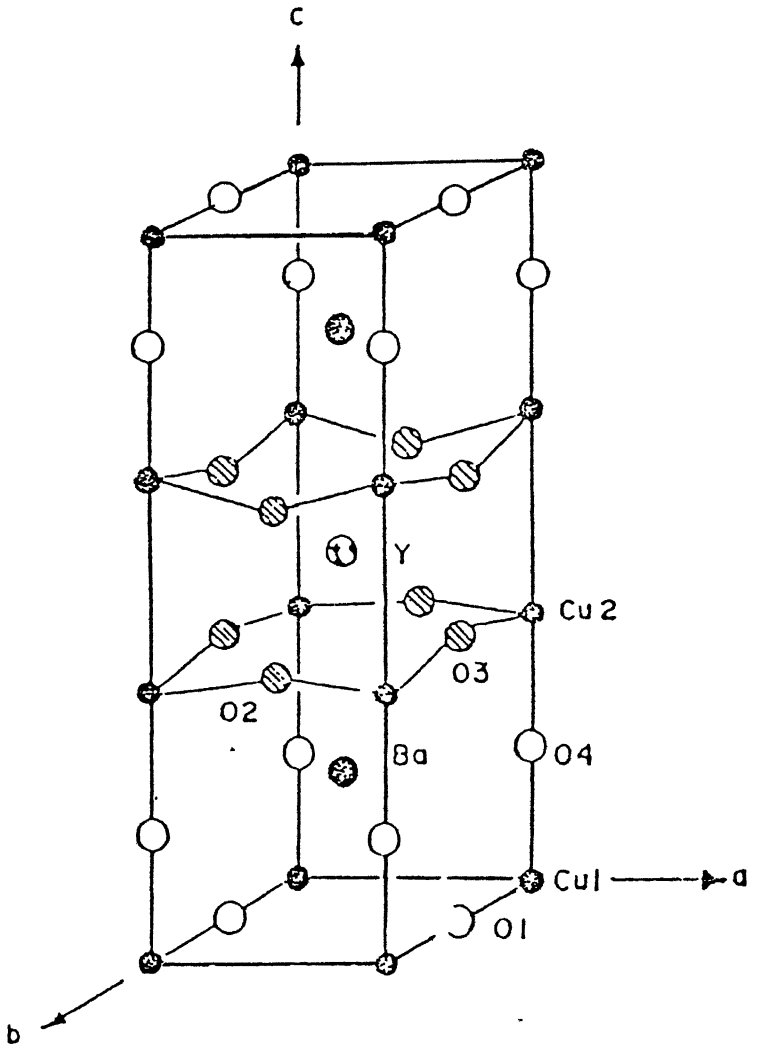

FIG. 1.9 CRYSTAL STRUCTURE OF $YBa_2Cu_3O_{7-x}$ [REF. 47]

between $YBa_2Cu_3O_7$ and $YBa_2Cu_3O_6$ is given in Table 1.4. The bond angles are presented in Table 1.5.

The Cu(I)-O(4) distance of 1.795 A^o is significantly shorter and that for Cu(2)-O(4) of 2.469 A^o is significantly longer in $YBa_2Cu_3O_6$. The other interatomic distances are changed only slightly. These changes make Cu(I) two coordinate and suggest that $YBa_2Cu_3O_6$ as reflected by the long bond distance and the shifting of Cu(2) closer to the plane of O(2) atoms, 0.21 A^o compared to 0.28 A^o in $Ba_2YCu_3O_7$. The unexpected short Cu(1)-O(4) bond distances in $Ba_2YCu_3O_7$ suggests, on the basis of bond strength calculations, that this site is preferentially occupied by the Cu^{3+} ions present in the structure and the suggested formula for $Ba_2YCu_3O_7$ should be $YBa_2Cu_3^{3+}Cu_2^{2+}O_7$. Thus the structure of $Ba_2YCu_3O_x$ is best described as containing localised Cu^{1+} and Cu^{3+} (Cu^{1+} at x=6 and Cu^{3+} at x=7). Pande et al [ref. 25] reported that in tetragonal phase, the oxygen and oxygen valancies (V) are distributed randomly and a=b. The CuO basal plane can undergo ordering wave instabilities so that on orthorhombic phase, the oxygen and V are ordered, resulting in one dimensional Cu-O chains parallel to the a - axis and Cu-V chains parallel to b-axis with a<b. The high T_c is attributed to these chains.

1.3.3 Oxygen Stoichiometry and Orthorhombic - to- Tetragonal Transition in $YBa_2Cu_3O_{7-x}$

Elucidation of the nature of the oxygen on stoichiometry is crucial to a detailed understanding of the electronic properties including superconductivity. Gallagher et al [ref. 29] reported

that the $YBa_2Cu_3O_x$ Perovskite compound is stable either in the tetragonal or in the orthorhombic phase depending on oxygen content x. The tetragonal phase has a lower oxygen content (x< 6.5-6.6) and it is stable at high temperatures. The tetragonal phase is a non-superconducting phase. On the otherside, orthorhombic phase contains more oxygen (x>6.5-6.6) and becomes superconducting at or below 90-95 K.

Table 1.2 : Fractional Atomic Coordinates in $YBa_2Cu_3O_7$ [Ref. 42]

Atom	x	y	z
Y	0.5000	0.5000	0.5000
Ba	0.5000	0.5000	0.1850(2)
Cu(1)	0.0000	0.0000	0.0000
Cu(2)	0.0000	0.0000	0.3565(5)
O(1)	0.0000	0.5000	0.0000
O(2)	0.0000	0.0000	0.1566(23)
O(3)	0.5000	0.0000	0.3776(21)
O(4)	0.0000	0.5000	0.3765(21)

Table 1.3 : Fractional Atomic Coordinates in $YBa_2Cu_3O_6$ [Ref. 42]

Atom	x	y	z
Y	0.5000	0.5000	0.5000
Ba	0.5000	0.5000	0.1952(2)
Cu(1)	0.0000	0.0000	0.0000
Cu(2)	0.0000	0.0000	0.3607
O(1)	0.0000	0.0000	0.1518(2)
O(2)	0.0000	0.5000	0.3791(1)
O(4)	0.0000	0.5000	0.0000

Table 1.4 : Bond Distance in $YBa_2Cu_3O_7$ and $YBa_2Cu_3O_6$ [Ref. 42]

$YBa_2Cu_3O_7$		$YBa_2Cu_3O_6$	
a = 3.8198(1) A^o		a = 3.8570 (1) A^o	
b = 3.8849(1) A^o		c = 11.8194(3) A^o	
c = 11.6762(3) A^o			
Bond	Distance (A^o)	Bond	Distance (A^o)
Ba - O(4)	2.7408 (4)	Ba-O(4)	2.7751 (5)
Ba - O(2)	2.984 (2)	Ba - O(4)	2.7751 (5)
Ba - O(3)	2.960 (2)	Ba - O(2)	2.905 (1)
Ba - O(1)	2.874 (2)		
Ba - O(5)	2.895 (2)	B - O(2)	2.1004 (8)
Y - O(2)	2.469 (1)		
Y - O(3)	2.886 (1)	Cu(1) - O(4)	1.795 (2)
Cu(1) - O(4)	1.816 (2)	Cu(2) - O(4)	2.469 (2)
Cu(1) - O(1)	1.9429 (1)	Cu(2) - O(2)	1.9406 (3)
Cu(2) - O(4)	2.295 (3)		
Cu(2) -O(2)	1.9299 (4)		
Cu(2) - O(3)	1.9667 (4)		

Table 1.5 : Bond Angles in $YBa_2Cu_3O_7$

Bond	Angle (deg.)
O(1) - Cu(1) - O(I)	180
O(1) - Cu(1) - O(4)	90
O(2) - Cu(2) - O(3)	88.96
O(2) - Cu(2) - O(4)	98.14
O(3) - Cu(2) - O(4)	97.42

The tetragonal-to-orthorhombic transition is a reversible process and the transition temperature depends on the ambient oxygen partial pressure. Fig. 1.10 shows the variations of transition temperature with respect to oxygen partial pressure. Schuller et al [ref. 30] and Murphy et al [ref. 31] reported transition temperatures in pure oxygen of 750°C and 686°C respectively where as in air, temperatures of 610°C and 575°C have been reported. Badwal et al [ref. 32] reported that the tetragonal-to-orthorhombic transition occurs at 675-680°C in 100% O_2 615-625°C in air and 570-580°C in 5% O_2.

At the orthorhombic-to-tetragonal transition the a-axis (tetragonal) becomes nearly half of the a and b axis (orthorhombic) and the c-axis becomes elongated resulting in a volume increase. Fig. 1.11 and 1.12 shows the variation of Lattice parameters and volume with temperature and oxygen content respectively. The expansion along c is nearly double that along a (17.6 vs. $9.6 \times 10^{-6}/^{\circ}C$) with in the tetragonal unit cell. The volume change, $\Delta V/3V$, in average cell dimensions at 25°C for the T and O structures is 0.483%.

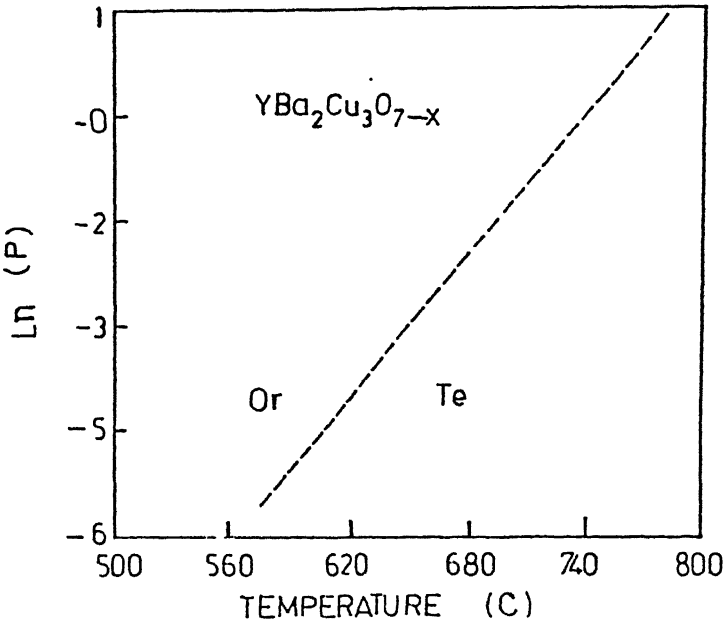

FIG. 1.10 THE VARIATION IN THE ORTHORHOMBIC (Or) TO TETRAGONAL (Te) PHASE TRANSITION TEMPERATURE AS A FUNCTION OF OXYGEN PARTIAL PRESSURE [REF. 32]

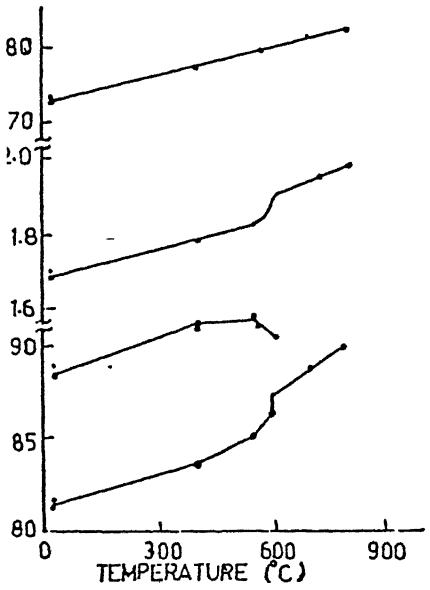

1.11 LATTICE PARAMETERS vs. TEMPERATURE FOR $Ba_2YCu_3O_X$ IN AIR [REF. 29]

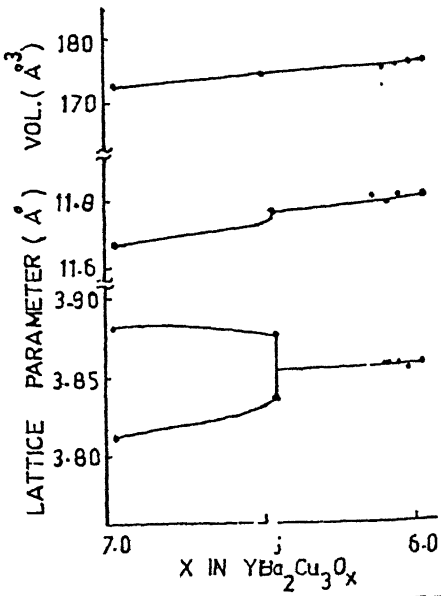

FIG. 1.12 LATTICE PARAMETERS vs. OXYGEN STOICHIOMETRY FOR $Ba_2YCu_3O_X$ [REF. 29]

The superconducting properties of $YBa_2Cu_3O_{7-x}$ very mu depends upon the oxygen content i.e., on the value of x. T superconducting transition temperature decrease as the oxyg content decreases and this is clearly shown in Fig. 1.13. Th transition is very sharp when the oxygen content is close to This can be seen from the Fig. 1.14 which gives the temperatu dependence of magnetisation. For x=0 the transition is very sha and it becomes broader as the x value increases.

1.3.4 Synthesis

Bulk superconductors can be synthesized by various routes solid state reactions [ref. 33, 34], solution techniques [ref. 35 36], and oxidation of metallic precursors that contain require metallic constituents [ref. 37] only solid state reactior technique is described here.

Solid State Reactions:

Perovskite oxides have traditionally been prepared by hig temperature solid state reactions of the binary oxides or suitabl oxide precursors such as carbonates, nitrates, oxalates, citrate etc.

$YBa_2Cu_3O_{7-x}$ can be prepared by handgrinding in a mortar an pestle or by ballmilling the proper proportions of oxides o carbonates i.e. CuO, Y_2O_3, $BaCO_3$ (or Ba_2O, $Ba(NO_3)_2$). The powde should be predried in an oven to remove any absorbed moistur prior to weighing. Y_2O_3, $BaCO_3$, CuO should be taken in the rati 0.5:2:3 and mixed thoroughly to ensure a homogeneous mixture. Th mixed powders are then calcined at 900-950^{o}C in air or oxyge atmosphere. In the calcining step carbonates decompose to th oxides and CO_2, and a multicomponent oxide is formed i.e.,

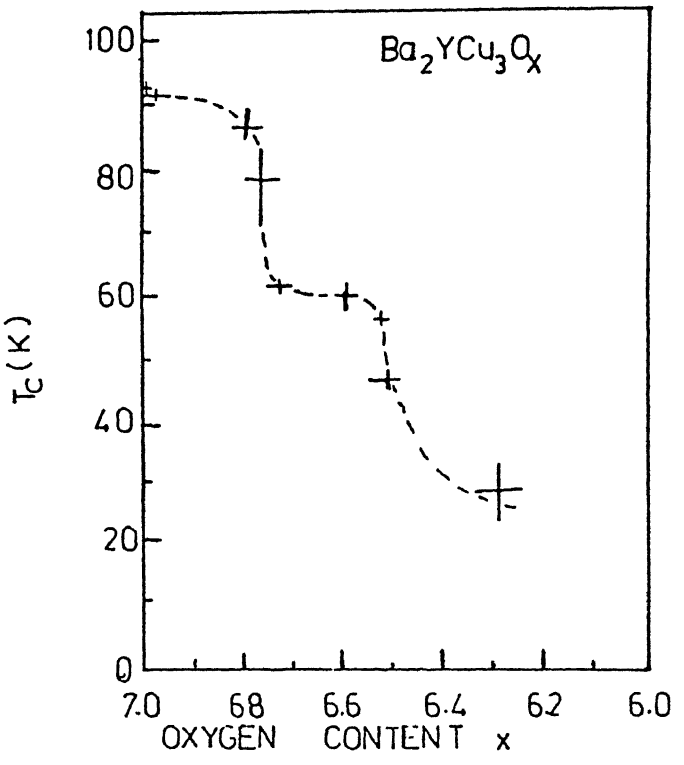

FIG. 1.13 CRITICAL TEMPERATURE AS A FUNCTION OF x IN $YBa_2Cu_3O_x$ [REF. 27]

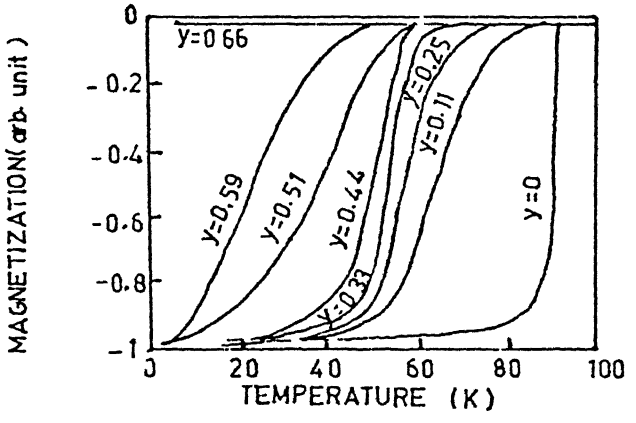

FIG. 1.14 EFFECT OF OXYGEN CONTENT ON THE TEMPERATURE DEPENDENT MAGNETIZATION FOR $YBa_2Cu_3O_{7-x}$ [REF. 33]

$$\frac{1}{2}\ Y_2O_3 + 2BaCO_3 + 3\ CuO \longrightarrow YBa_2Cu_3O_{6.5} + 2CO_2 \uparrow$$

The above formula assumes no addition or depletion of oxygen from ambient during the calcining step, an assumption not always true. $BaCo_3$ decomposes to BaO at very high temperatures above 1300°C, however, in the presence of CuO the decomposition starts at 800°C. But the decomposition at this temperature is very sluggish and requires several days. The decomposition rate can be increased by increasing the calcining temperatures. However, temperature above 950°C deteriorates the superconducting properties. The calcined powders are pelletised and sintered at about 950°C. The sintered samples are slowly cooled in flowing oxygen. To attain the oxygen stoichiometry close to O_7 often the samples are to be annealed in flowing O_2 at 400 - 600°C. During annealing in flowing O_2 the following reaction takes place:

$$Y_1Ba_2Cu_3O_{6.5} + \frac{\delta}{2}\ O_2 \longrightarrow Y_1Ba_2Cu_3O_{6.5+\delta}$$

It was found that the $BaCO_3$ remained undecomposed or regenerated in minor amounts after calcination and sintering [ref. 38]. Often the calcination and sintering steps would be repeated 2 - 3 times to obtain a single phase $YBa_2Cu_3O_{7-\delta}$. A careful processing steps are required to obtain optimal quality superconductors. It is important to heat the powder mixture rapidly to temperatures above 900°C, where $YBa_2Cu_3O_{7-\delta}$ is dominant phase. Decomposition at lower temperatures than 900°C leads to the formation of substantial quantities of impurity phases such as $BaCuO_2$ and Y_2BaCuO_5. Temperatures higher than 970°C result in a multiphase mixture including Y_2BaCuO_5. In addition 1-2-3 compound reacts with most crucible materials including silica, and Alumina.

Zirconia and gold are relatively inert. The impurities present in the 1-2-3 superconductor result in a poor grain-to-grain contact, hence reducing the critical current density (J_c). Using high purity starting materials, maintaining starting cation ratio and maintaining high intimacy of mixtures yields a pure single phase superconductors.

Some of the problems normally associated with this process are:

(i) Agglomerates in calcined powders are usually larger than 25μm, producing ceramics which are highly porous and may have poor mechanical properties.

(ii) Inadequate mixing of powders can lead to compositional inhomogeneities, inadequate stoichiometry control, the production of extraneous phases.

1.3.5 Characterization of Y-Ba-Cu-O Superconductors

1.3.5(i) Magnetic Susceptibility:

The fraction of a sample that is superconducting can be determined from the magnetic susceptibility measurements. A superconductor in low magnetic fields behaves as a perfect diamagnet and has a susceptibility (in Gaussian units) of $-1/4\pi$); comparing the measured moment against this value for an ideal superconductor gives a good estimate of how much of the sample is superconducting. Fig. 1.15 shows the susceptibility curve for a single phase and multiphase 1-2-3 superconducting samples. It can be seen from the figure that the transition is sharp in single phase material than in the multiphase material.

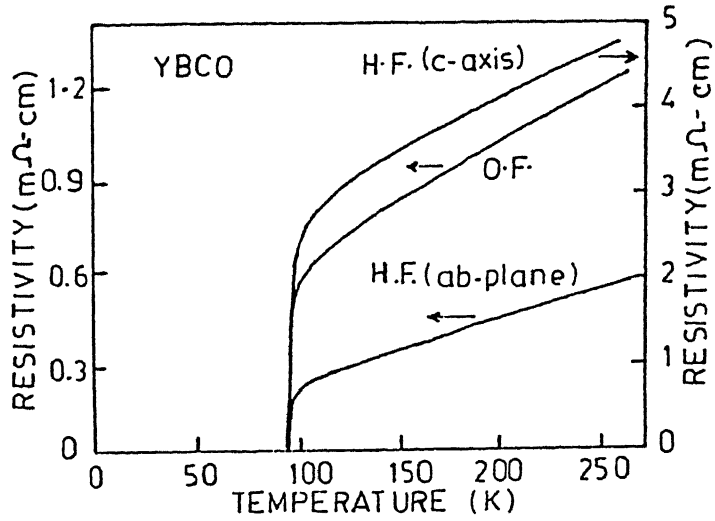

FIG. 1.20 TEMPERATURE DEPENDENCE OF RESISTIVITY FOR GRAIN ORIENTED (H.F.) AND NON ORIENTED (O.F.) YBCO CERAMICS [REF. 12]

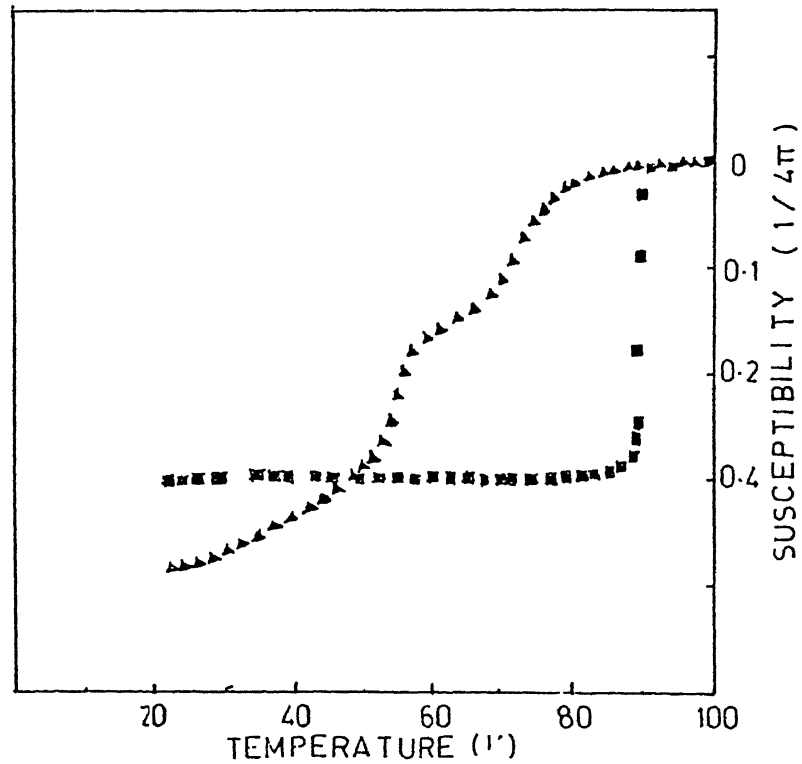

FIG. 1.15 TEMPERATURE DEPENDENCE OF SUSCEPTIBILITY FOR Y $Ba_2Cu_3O_{7-x}$ [REF. 51] IN 0.01 G. FIELD (■) SINGLE PHASE (▲) MULTI PHASE

1.3.5(ii) Electrical Resistivity:

At the critical temperature of an ideal superconductor the electrical resistivity suddenly drops to zero, but the transition in the oxide superconductors is very wide - as the temperature is lowered, an appreciable decrease in the resistivity starts well before the zero resistance state is obtained.

A conservative estimate for the critical temperature, called the mid pointT_c, is the point in the resistivity curve at which the resistivity has dropped to half the value extrapolated from the high temperature behaviour. It is also useful to know the temperatures at which the resistivity has dropped by 10% and 90% respectively, for these give an estimate of how wide the transition is and whether it is symmetric about the mid point. The mid point T_c is usually much lower than the onset T_c, the temperature at which the resistivity first begins to deviate from its behaviour at high temperatures.

Electrical resistivity of $YBa_2Cu_3O_{7-x}$ super conducting samples is normally measured by a four probe resistivity meter. Temperature dependence of electrical resistivity of a sintered sample is shown in Fig. 1.16. At room temperature resistivity is 600-700$\mu\Omega$-cm and decreases to 200-250$\mu\Omega$-cm at 100 K. Fig. 1.17 shows the effect of magnetic field on resistance. The resistance drop is shifted towards lower T.

Electrical resistivity of supeconducting samples greatly dependent on processing conditions. Fig. 1.18 shows the resistivities for samples sintered in three different states. It can also be seen that sintering in O_2 improved the electrical properties. The electrical resistivity also depends on the Rate

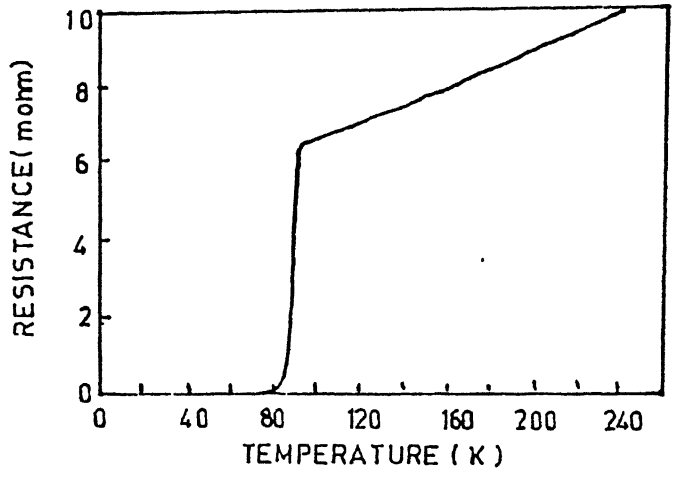

FIG. 1.16 TEMPERATURE DEPENDENCE OF RESISTANCE [REF. 4]

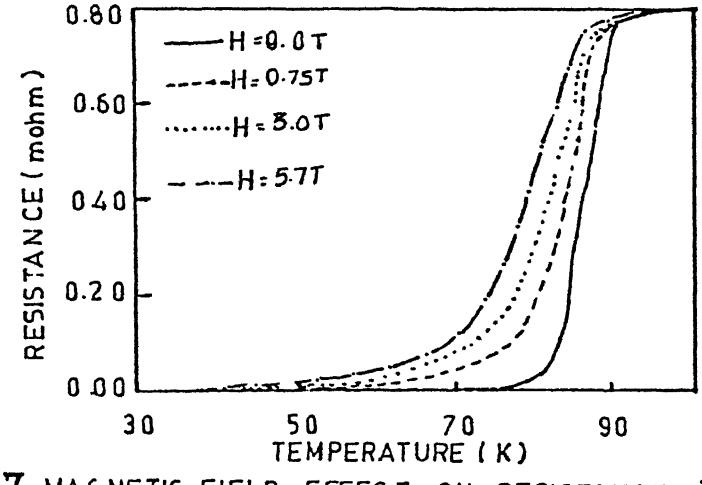

FIG. 1.17 MAGNETIC FIELD EFFECT ON RESISTANCE [REF. 4]

of Cooling and furnace atmosphere. Fig. 1.19 shows resistance vs temperature plots for different preparative conditions. From the figure it is clear that slow cooling and annealing in Oxygen gives better superconducting properties.

$YBa_2Cu_3O_{7-x}$ superconductors shows anisotropy in properties. Fig. 1.20 shows temperature dependence of resistivity of grain-oriented and unoriented samples [ref. 12]. The resistivity along the ab planes is lower than along the c-axis.

1.3.5(iii) X-ray Diffraction:

It is a well known fact that $YBa_2Cu_3O_{7-x}$ exists in two forms, superconducting orthorhombic phase and non-superconducting tetragonal phase. Fig. 1.21 shows the typical X-ray diffraction patterns of tetragonal and orthorhombic phases [ref. 40]. Gradual change of T to O structure by cooling $YBa_2Cu_3O_{7-x}$ can be observed by peak shift at $\sim 32^{o}$ as shown in Fig. 1.22. The impurity phases can be identified by examining the XRD pattern. The XRD also indicates orientation of grains in the sample and orientation factor can be evaluated by knowing the intensities of peaks.

1.3.5(iv) Estimation of Oxygen Stoichiometry:

The oxygen stoichiometry x in $YBa_2Cu_3O_x$ samples can be estimated by Thermogravimetric analysis (TGA) and iodometric titrations. Apart from accuracy of TGA it is found to be more useful when determining the effect of various gases on the oxygen content and on 123 phase formulation or decomposition.

1.3.6 Preferred Orientation in YBa-Cu-O Superconductors

Practical superconductors must possess very high, critical current density (J_c), order of 10^5-10^6 A/cm^2, for electrical applications. The bulk $YBa_2Cu_3O_{7-x}$ superconductors have critical

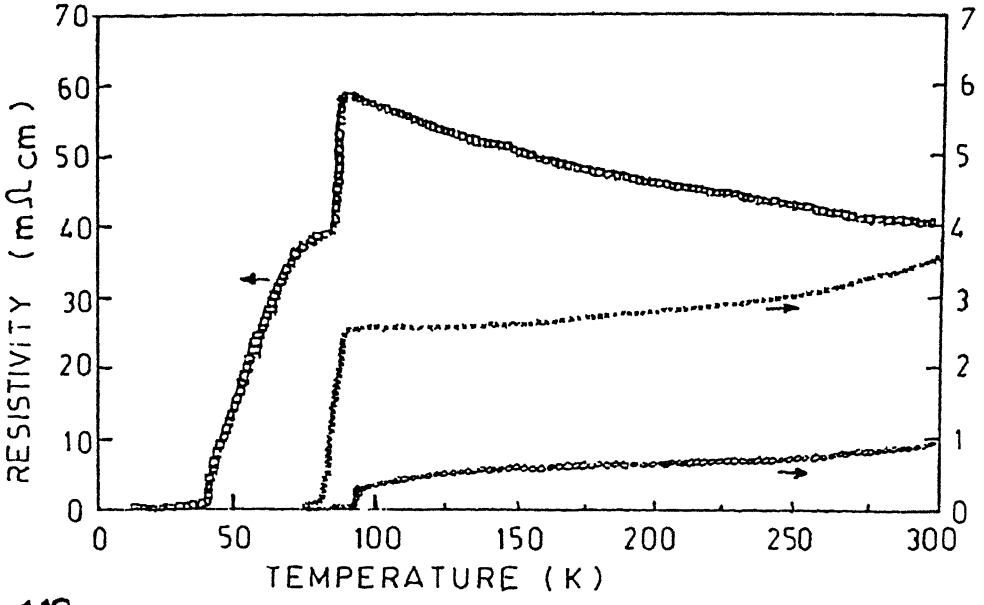

FIG. 1.18 RESISTIVITY vs. TEMPERATURE FOR A SAMPLE AT THREE DIFFERENT SINTERED STATES [REF. 50]
(□) TWICE SINTERED IN AIR AT 900°C FOR 12 HRS. AND 800°C FOR 40 HRS. (×) AN ADDITIONAL SINTERING IN AIR AT 900°C FOR 40 HRS. (○) RESINTERING AT 894°C FOR 4 HRS. IN A FLOW OF OXYGEN

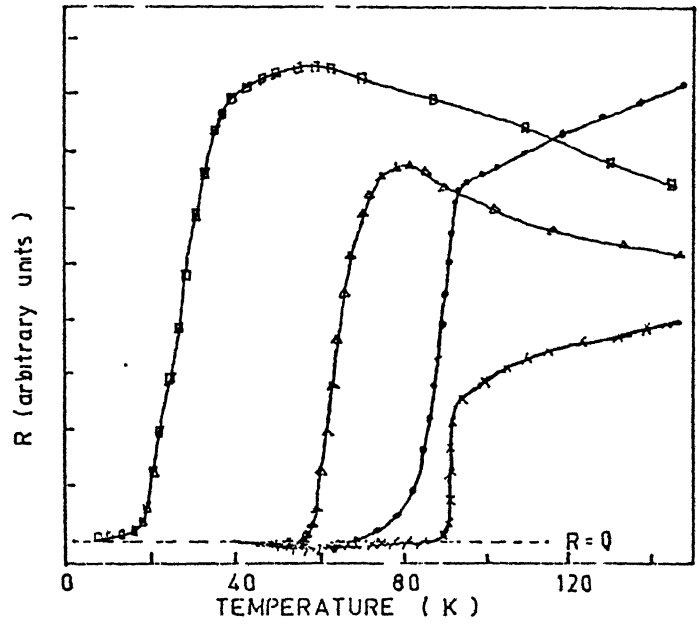

FIG. 1.19 RESISTANCE vs. TEMPERATURE PLOTS FOR DIFFERENT PREPARATIVE CONDITIONS. (□) FAST COOL O_2 ANNEAL. (▵) INTERMEADIATE COOL O_2 ANNEAL (•) SLOW COOL AIR ANNEAL (×) SLOW COOL O_2 ANNEAL [REF. 49]

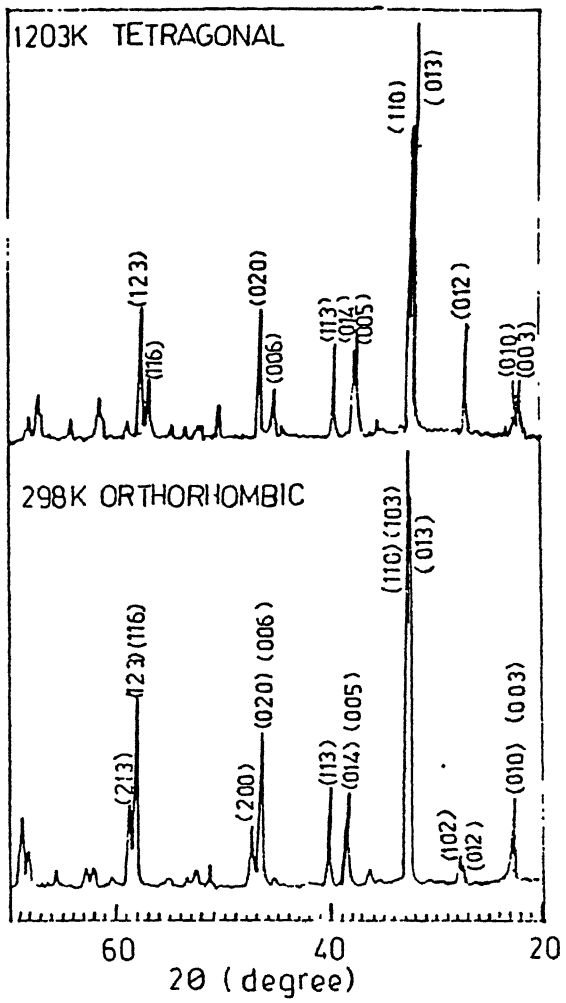

FIG. 1.21 POWDER X-RAY PATTERNS OF $YBa_2Cu_3O_x$ AT 1203K AND AT ROOM TEMPERATURE [REF. 43]

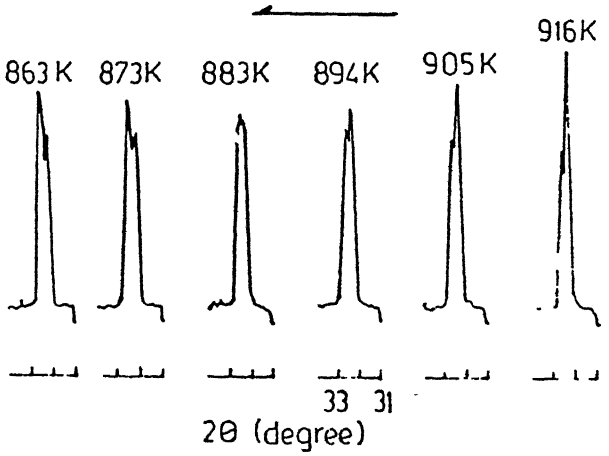

FIG. 1.22 PEAK SHIFT OF X-RAY DIFFRACTION OF $YBa_2Cu_3O_x$ ON COOLING [REF. 48]

current density about 10^1- 10^3 A/cm^2.

There are in essence, two principal issues that determine J_{ct} [critical transport current density]. The first and most critical is the tendency of high-temperature superconducting materials to be only weakly coupled across the grain boundaries of bulk, poly crystalline samples. This is called "weak-link or granularity problem". In this state, J_{ct} is much less than the local J_c in the flux-pinning regions [ref. 41]. The second issue is the need to develop strong flux pinning, so that the fluxoids of the mixed superconducting state can resist the Lorentz force.

Grain orientation improves grain-to-grain contact and thus enhances the critical current density. Grain oriented bulk polycrystals of YBCO can be synthesized by hot pressing [ref. 9,13,16], press forging [ref. 12,14], melt method [ref. 15] and by a field orientation methods [ref. 11].

Fig. 1.23 shows the resistance vs. temperature measurements in hot pressed $Ba_2YCu_3O_{7-x}$ ceramics. Higher the hot-pressing pressure lower the room temperature resistivity Fig. 1.24 shows the x-ray diffraction patterns of hot-forged and ordinarily fired $YBa_2Cu_3O_{7-x}$ ceramics. It is reported that the J_c [= 110 a/cm^2] of the grain oriented (H.F.) sample was elevated to one and a half time [=74 A/cm^2] that of non oriented sample.

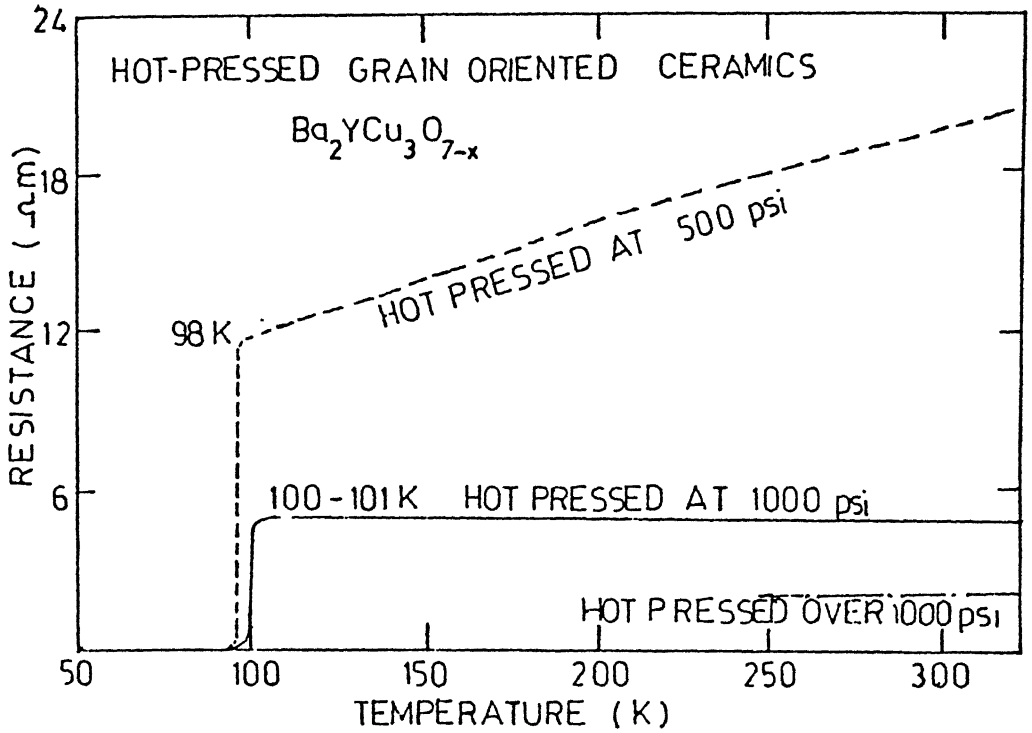

FIG. 1.23 RESISTANCE vs. TEMPERATURE MEASUREMENTS IN HOT-PRESSED $Ba_2YCu_3O_{7-x}$ CERAMICS [REF. 10]

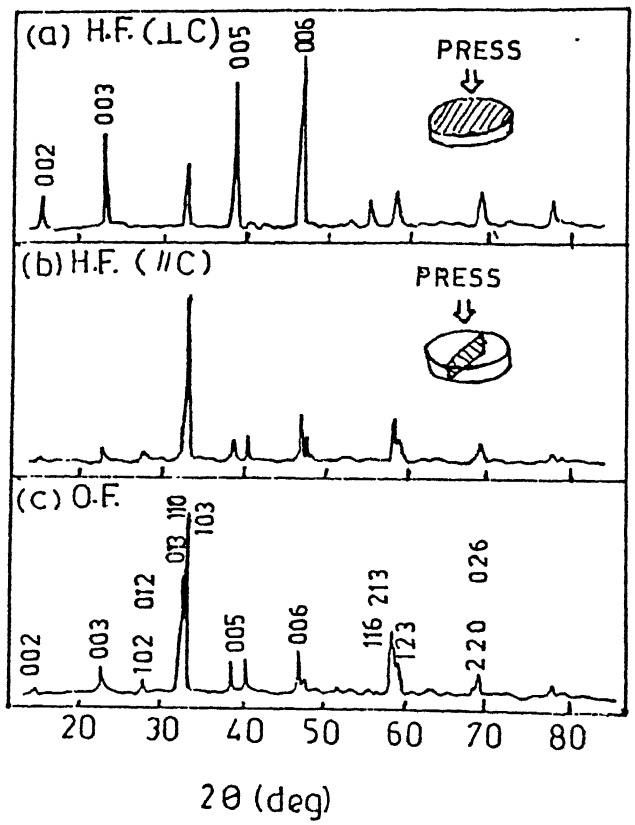

FIG. 1.24 X-RAY DIFFRATION PATTERNS OF HOT-FORGED (H.F.) AND ORDINARILY FIRED (O.F.) YBCO CERAMICS [REF. 12]

CHAPTER - II

EXPERIMENTAL PROCEDURE

The present investigation involved production of high-temperature YBCO superconductors by solid state reactions technique and subsequent characterization. The experimental procedures followed and the techniques used for characterization are as described in the following sections.

2.1 Furnace Details

Formation of superconducting phase, $YBa_2Cu_3O_{7-x}$ needs presintering, sintering and annealing (in air or Oxygen atmosphere) treatments. The sintering temperatures required are 900 - 950^{o}C. The sintering periods vary from few hours to few days. These conditions can be easily met in the laboratory using a furnace having KANTHAL heating element. A tubular furnace with KANTHAL heating element has been used for this purpose.

The furnace is connected to power supply with a controlling panel. The panel contained a variac, temperature controller/indicator (ON/OFF type) and a relay. A Pt vs. Pt + 10%. Rh Thermocouple is employed for the temperature measurement. A quartz tube of 1" diameter and 48" length, thoroughly cleaned with HF acid is employed as a working tube.

The furnace is then calibrated using a reference thermo couple at different temperatures for different time periods. A constant temperature zone of length ~ 49 mm, is determined.

2.2 Die Design and Fabrication

For cold pressing 304 stainless steel dies are used. Fig. 2.1 shows the dimensions of the fabricated die. A slight tapering was made on the bottom side of the die for a length of about 2 cm

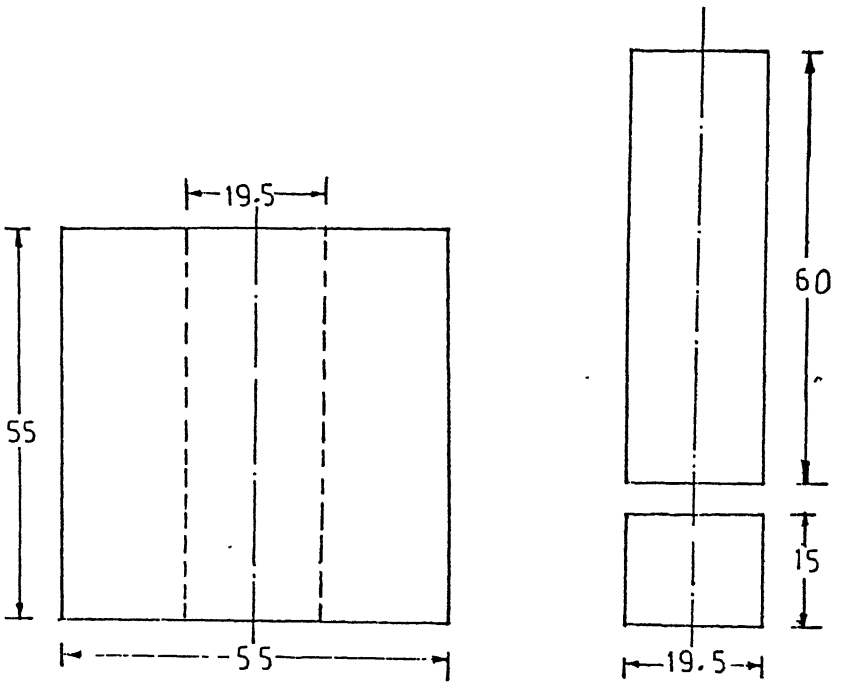

FIG. 2.1 COLD PRESSING DIE

C - COLLIMATOR

S - SAMPLE

F - FILM

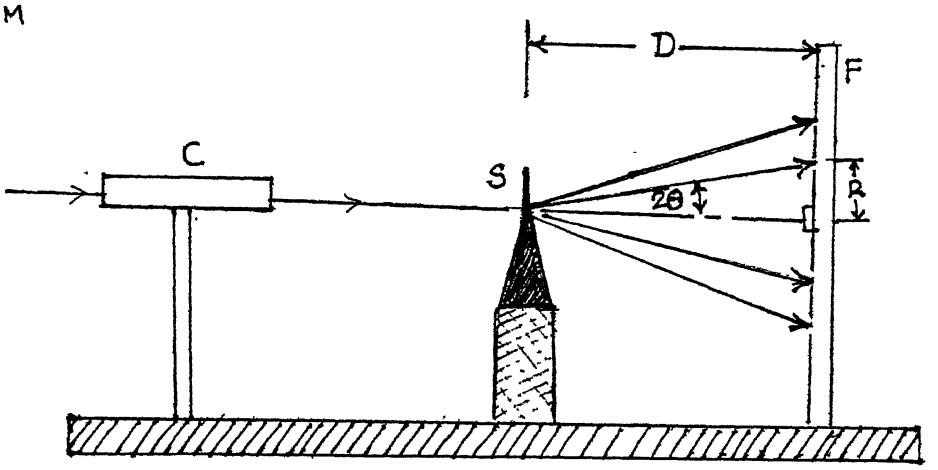

$$\text{Tan } 2\theta = \frac{R}{D}$$

FIG. 2.3 SCHEMATIC ARRANGEMENT OF SAMPLE ON A TRANSMISSION LAUE CAMERA

to facilitate easy removal of the pellet.

2.3 Synthesis

2.3.1 Raw Materials: To prepare a good superconductor purity of the raw materials plays a stellar role. For that reason, high purity (>99.5 pct) raw materials Y_2O_3, $BaCO_3$ and CuO powders were taken. Particle size analysis of powdered mixture is done by using **Coulter Counter Model Z_B and B.** It is found that the particle size essentially varies from 1.5 μm to 17.0 μm and further, the maximum portion (>60 pct. by wt.) of which is in the range of 6.5 μm to 13.5 μm.

2.3.2 Mixing : The raw materials are predried. Initially, to eliminate any moisture, for a period of 6 hours at 125°C. Then the powders of Y_2O_3, $BaCO_3$ and CuO are weighed in the mole ratio of 0.5:2:3. The weighed powders are then mixed thoroughly in an Agate ball mill for 24 hours in acetone medium. The mixture is dried completely.

2.3.3 Presintering and Sintering : The dried mixture is then pelletised at 1000Kg/cm^2 pressure for pre-sintering. The presintering is carried out at 925°C for 24 hours in air. These presintered pellets were reground and sintered at 930°C for 24 hours in flowing oxygen atmosphere. The compaction pressure used for making pellets for sintering is 1500 Kg/cm^2. The sintered pellets are annealed at 425°C for 10 hours during cooling in flowing oxygen atmosphere. Three batches of samples are produced with similar conditions. These are designated as CA_1, CA_2 and CNR_3 for identification.

To study the effect of compaction pressure on the sintered densities some samples are cold compacted at 1550, 2260, 3120,

3818, 4640 and 5214 Kg/cm^2. All these samples are sintered at 930^{o}C for 20 hours and annealed at 500^{o}C for 10 hours in flowing Oxygen.

To investigate the effect of heating rate on sintered density, some presintered samples are cold pressed at 3500 Kg/cm^2 pressure. All the samples are heated at 10^{o}C/min upto 800^{o}C and then from 800^{o}C to 960^{o}C, different samples are heated at 10^{o}C/min, 2.5^{o}C/min and 1.0^{o}C/min respectively. Finally they are maintained at 960^{o}C for 24 hours in air.

2.3.4 **Annealing Treatment:** CA_1, CA_2, and CNR_3 samples are reannealed at 700^{o}C for 10 hours in the flowing oxygen. This treatment is repeated on few samples once more.

2.4 Characterization:

The samples produced as discussed above are characterized by x-ray diffraction (XRD), Differential thermal analysis (DTA), Scanning Electron Microscope (SEM), Electron Paramagnetic Resonance (EPR) measurements, and Pin hole Diffraction patterns.

2.4.1 **X-ray Diffraction Analysis:** X-ray diffraction studies are carried out in a RICH - SEIFERT ISO-DEBYE FLEX 2002 Diffractometer using Ni-filtered copper K_α radiation. The XRD is carried out both on pellets and powder samples. To ensure better resolution, slow scanning speeds are employed. The conditions set for taking diffraction patterns are given in Table 2.1.

Table 2.1 : Conditions set for tracing Diffraction patterns using ISO Debyeflex-2002 Diffractometer

Radiation	Ni-Filtered Cu K_α
Tube Voltage	30 KV
Tube Current	20 mA
Receiving Slit width	0.2 mm
X-ray slit width	2 or 3 mm
Scanning speed	$1\text{-}2^{o}$/min
Chart speed	30 mm/min
Time constant	3 sec
Intensity range	300 counts/sec
Angular range of scan	$20^{o} \leq 2\theta \leq 80^{o}$

The peaks are identified by comparing with the values of x-ray diffraction data available in the literature and the densities are determined from the sample dimensions and weight.

2.4.2 **EPR Measurements:** EPR measurements have been carried out on both the normal and the superconducting states of $YBa_2Cu_3O_{7-\delta}$ using VARIAN E-109, X-BAND Spectrometer. The resultant EPR Spectgra are shown in Fig. 3.4 and 3.5. The parameters used for tracing EPR spectrum are given below:

Table 2.2 Parameters used for Tracing EPR Spectrum

Scan Range	5 KG
Field Set	2500 G
Time constant	0.032 sec
Modulation amplitude	0.5 G
Modulation frequency	9.2Ghz
Temperature	Liquid Nitrogen (77K) and R T (300K)
Microwave power	0.5 mW
Receiver gain	2×10^{3}

2.4.3 **Differential Thermal Analysis:** Phase transformations, oxidation, reduction and melting are associated with enthalpy change. These changes are observed using differential thermal analysis. DTA is carried out on a Dupont 9900 Thermal Analysis - DTA1600 in air.

2.4.4 **Scanning Electron Microscopic Studies :** Presintered, sintered and grain oriented samples are examined using the JEOL 840A Scanning Electron Microscope. Spot analysis is done to determine the compositions of various phases using Energy Dispersive analysis of x-rays (EDAX) [Fig. 2.2].

2.4.5 **X-Ray Pin Hole Patterns:** From the x-ray diffraction measurements on YBCO superconductors, it is evident that there are no peaks present at $2\theta > 90^{o}$. Hence, it is not possible to obtain Back reflection Laue patterns. The transmission Laue patterns are taken using copper K_{α} radiation using a Nickel filter. Since the thickness through which x-rays pass through is of the order of few microns, coupled with the fact that superconducting samples are brittle, it is very difficult to obtain the thin sample. Hence the pin hole patterns are taken through one of the edges of the sample. Fig. 2.3 shows the schematic arrangement for taking pin hole transmission patterns.

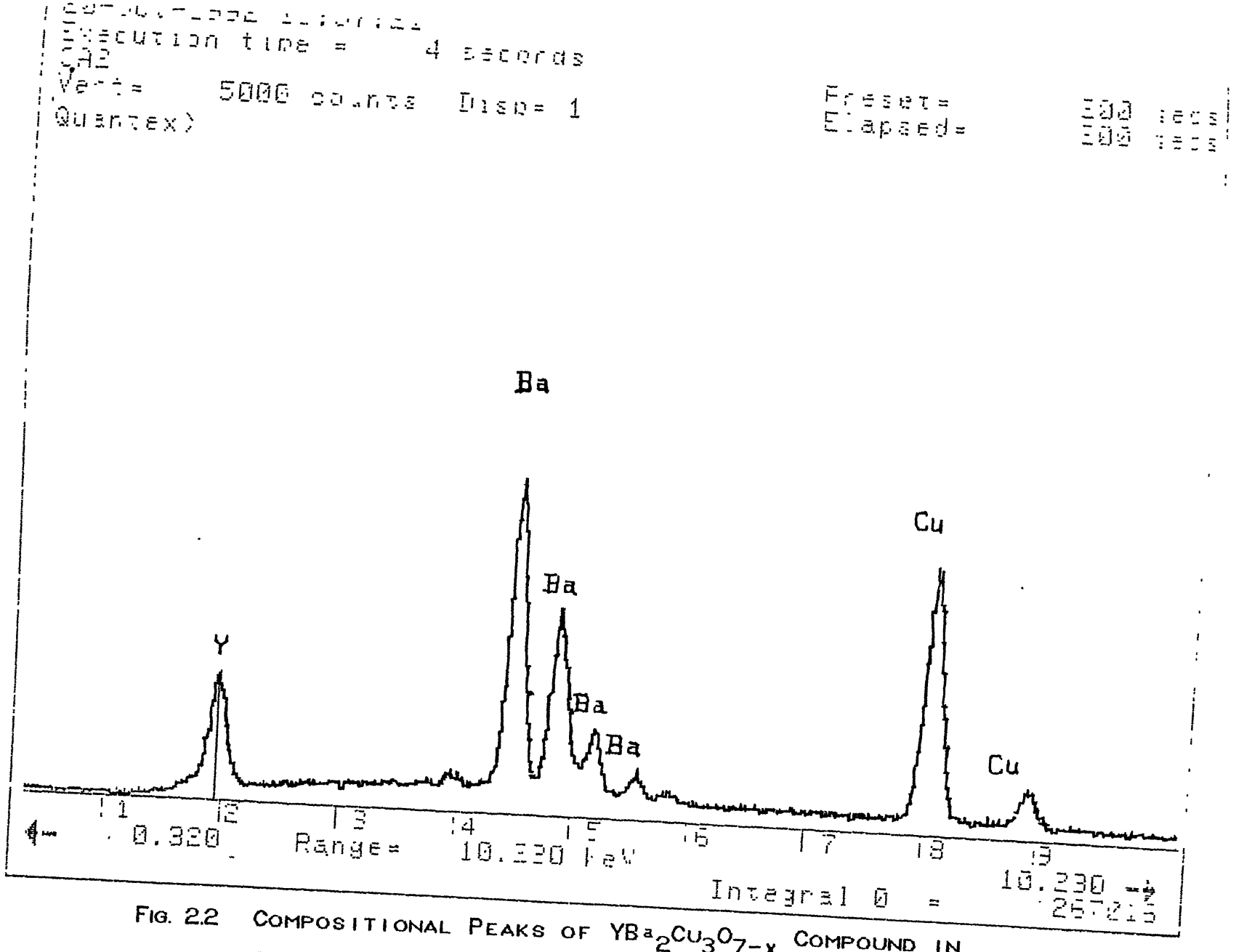

FIG. 2.2 COMPOSITIONAL PEAKS OF $YBa_2Cu_3O_{7-x}$ COMPOUND IN SEM-EDAX ANALYSIS

CHAPTER III

RESULTS AND DISCUSSIONS

3.1 Formation of $YBa_2Cu_3O_{7-x}$ Compound:

The formation of $YBa_2Cu_3O_{7-x}$ compound is studied using x-ray diffraction and Differential thermal analysis methods. Fig. 3.1(a) and 3.1(b) shows the x-ray diffraction patterns of presintered and sintered Y_2O_3, $BaCO_3$ and CuO mixture. During presintering and sintering the following reaction occurs to form $YBa_2Cu_3O_{7-x}$ superconducting phase.

$$\frac{1}{2}\ Y_2O_3 + 2BaCO_3 + CuO \longrightarrow YBa_2Cu_3O_x + 2CO_2 \uparrow$$

This reaction is complete only after second firing state, i.e. presintering. From Fig. 3.1(a) it can be seen that significant amount of $YBa_2Cu_3O_{7-x}$ is formed during presintering. The $BaCO_3$ decomposes above 1300°C when present alone. But when it is mixed with CuO the decomposition starts at 800°C. At this temperature the reaction is so sluggish that it takes longer time periods for completion. However, the decomposition rate can be increased by increasing temperature. It can also be seen from Fig. 3.1(a) that some $BaCO_3$ was left undecomposed or regenerated. During presintering at 925°C the $BaCO_3$ decomposes to BaO and CO_2/CO.

$$BaCO_3 \Leftrightarrow BaO + CO_2/CO$$

But this reaction is reversible and depends upon the CO/CO_2 partial pressures. However, the $BaCO_3$ is decomposed completely after sintering the presintered powder at 930°C in flowing oxygen. But some impurity phase like $BaCuO_2$ and unreacted CuO are present even after oxygen annealing while the powder x-ray diffraction of

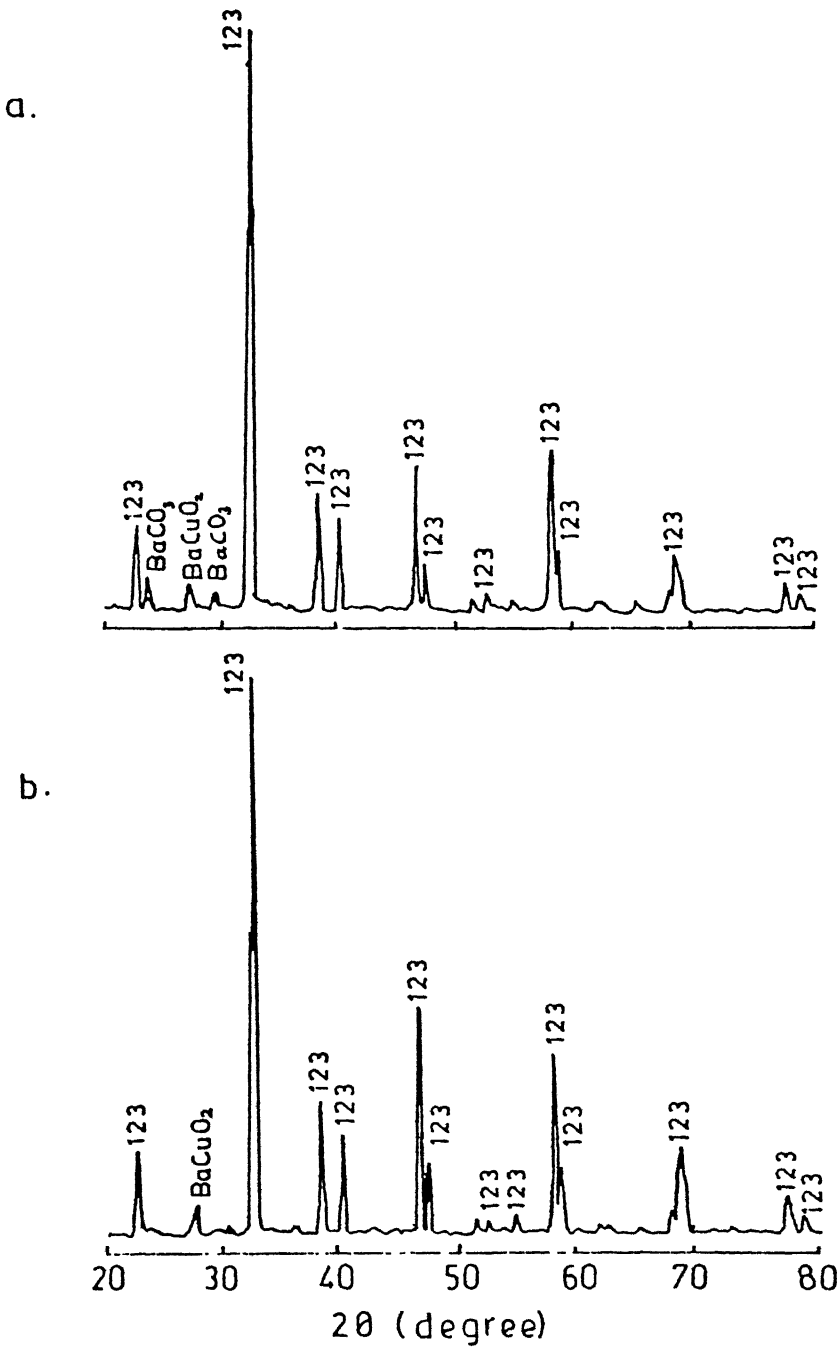

FIG.3-1 POWDER X-RAY DIFFRACTION PATTERNS OF (a) PRESINTERED AND (b) SINTERED $YBa_2Cu_3O_x$

sintered $YBa_2Cu_3O_x$ [Fig. 3.1(b)] indicates that the reaction has gone to completion, the DTA investigations showed the presence of traces of annealed precursors. Fig. 3.2 and 3.3 are the scanning electron micrographs which support the above analysis. X-Band EPR spectrum [Fig. 3.5] at 9.2GHz Modulation frequency and liquid Nitrogen temperature (77^oK) confirms the formation of Superconducting $YBa_2Cu_3O_{7-x}$ compound. This result is consistent with a recent report on the temperature dependence of the EPR for $YBa_2Cu_3O_{7-x}$ [ref. 43].

3.2 Sintering Studies:

The sintered microstructure is extremely process sensitive parameters such as sintering temperature and time, rate of heating and cooling, furnace atmosphere, particle size and size distribution have a major influence on sintered microstructure, but are not studied here.

D.T.A. analysis of unreacted mixed powders [Fig. 3.6] shows the γ to β transition of $BaCO_3$ at ~ 810^oC, followed by an endothermic reaction or melting, beginning at ~ 960^oC. The presintered mixture showed onset of liquid phase at ~880^oC and maximum at 960^oC. The onset of liquid phase occurs at higher temperatures ~930^oC after repeated reactions. This clearly shows that repeated reactions raised the onset temperature of the liquid phase.

In the D.T.A. curves the exothermic peaks at 275^oC shows that the Oxygen diffusivity is nil and above 275^oC only the oxygen diffusion occurs. This shows that the annealing temperatures should be above 275^oC. The peak at 550^oC indicates still higher mobility of Oxygen. This peak can be referred to phase transition

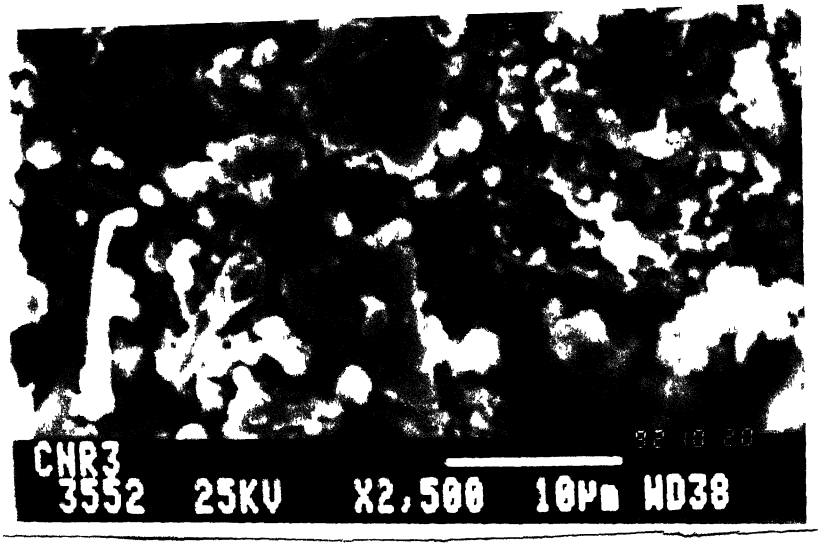

FIG. 3.2 SEM MICROGRAPH OF PRESINTERED (925°C, 24 HRS) GREEN COMPACT (MAGNIFIED FOUR TIMES)

FIG. 3.3 SEM MICROGRAPH OF SINTERED (930°C, 20 HRS AND ANNEALED AT 425°C FOR 10 HRS. IN OXYGEN) SAMPLE (MAGNIFIED FOUR TIMES)

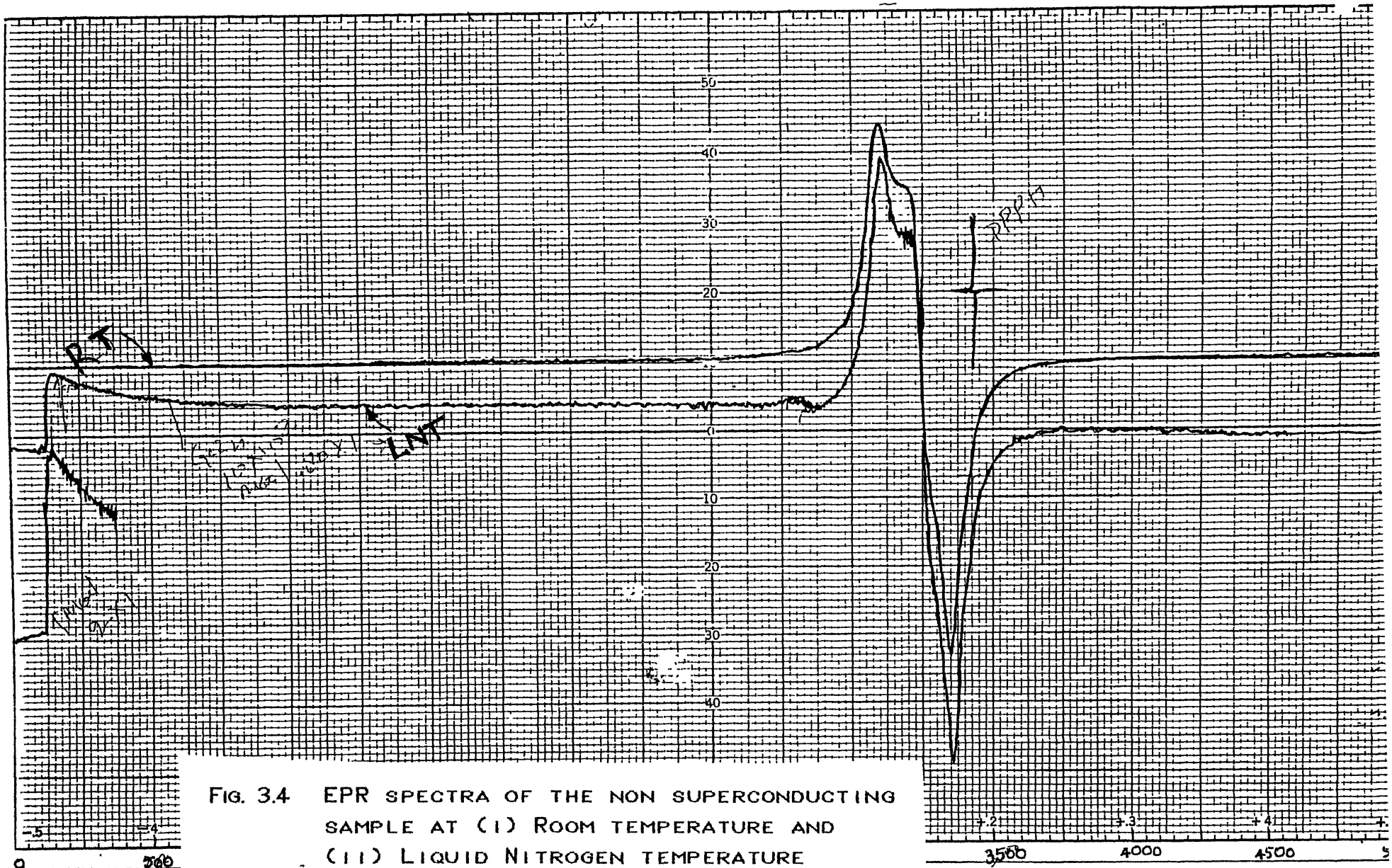

FIG. 3.4 EPR SPECTRA OF THE NON SUPERCONDUCTING SAMPLE AT (I) ROOM TEMPERATURE AND (II) LIQUID NITROGEN TEMPERATURE

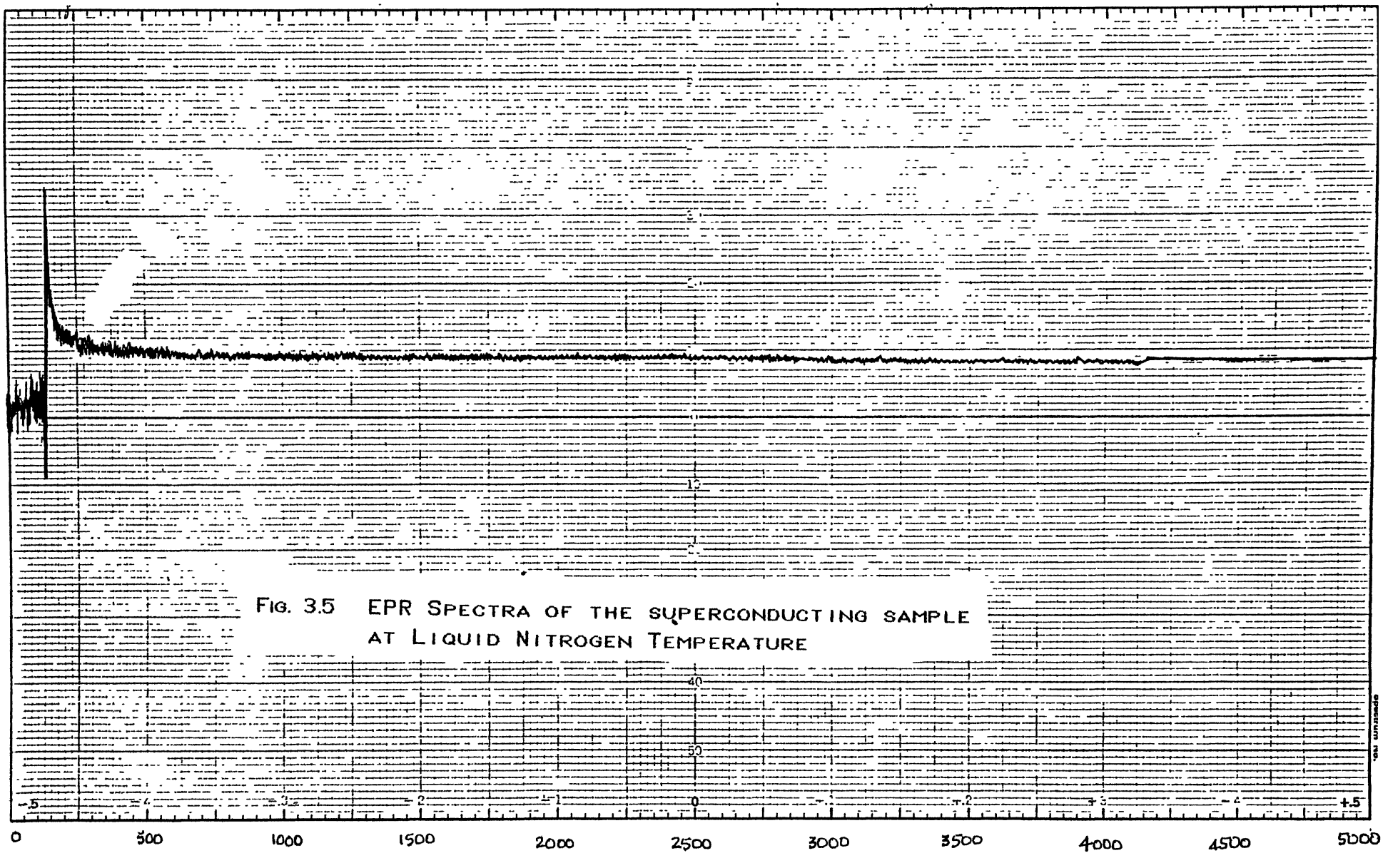

FIG. 3.5 EPR SPECTRA OF THE SUPERCONDUCTING SAMPLE AT LIQUID NITROGEN TEMPERATURE

from orthorhombic-to-tetragonal structure. The transition completes at 600°C. This value is in accordance with the reported values [ref. 30,31].

The density of the sample, compacted at 1560 Kg/cm^2, after sintering is 75% of the theoretical value (6.305 gm/cc). The densities are dependent on the compaction pressures. Table 3.1 gives the data on compaction pressure and densities. It can be seen that the densities increased with increasing compaction pressures. However after a critical value of compaction pressure cracks are formed in the green compact.

Effect of heating rate on sintered density (the heating rate dependence is due to liquid phase formation) is illustrated in Table 3.2.

Table 3.1 : Densities at different compaction pressures

Compation Pressure Kg/cm^2	Density (% theoretical)
1550	75
2260	80
3120	82
3818	88
4640	88
5214	Cracks developed in the green compact

Table 3.2 Effect of heating rate on sintered density

(The heating rate is due to liquid phase formation*)

Heating rate from 800°C to 960°C (°C/min)	Density (gm/cc)	% of theoretical Density**
10	5.5	81
2.5	5.86	85
1.0	5.86	85

* Heating rate to 800 C°– 10 C°/min

** Theoretical Density = 6.305 gm/cm

3.3 Analysis of Laue Patterns:

Fig. 3.7 and 3.8 shows the Laue transition patterns taken on sintered samples with similar conditions, but for different time periods. The former one is taken for 8 hours and while the latter one is for 11 hours. Such a longer exposures were needed because of poor quality films. From the figures it is clear that as the time of exposure increases the number and sharpness of peaks improved. Also, new peaks are observed [Fig. 3.7]. Presence of discontinuous rings or spotty in appearance suggesting that enough crystals are not present in the irradiated volume of the specimen to reflect all parts of the ring. Broadening of some rings infers the presence of very fine particles (< 1 μm).

Peaks corresponding to the (123) superconducting phase and impurity phases are identified from the powder diffraction patterns. Table 3.3 gives the transmission pinhole pattern analysis.

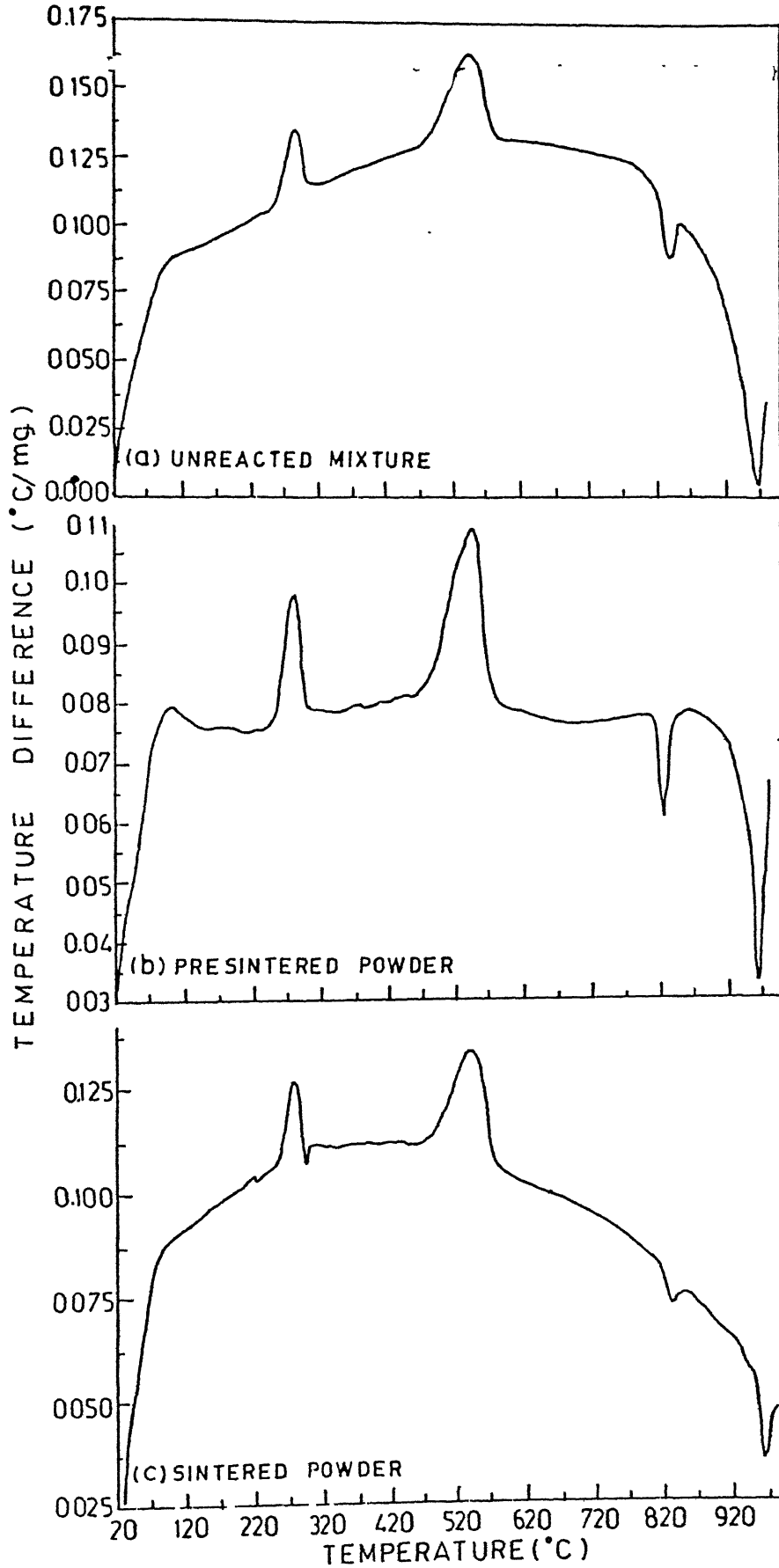

FIG 3.6 DTA CURVES OF 123 MIXTURES (Heating Rate 10°C/Min., in air)

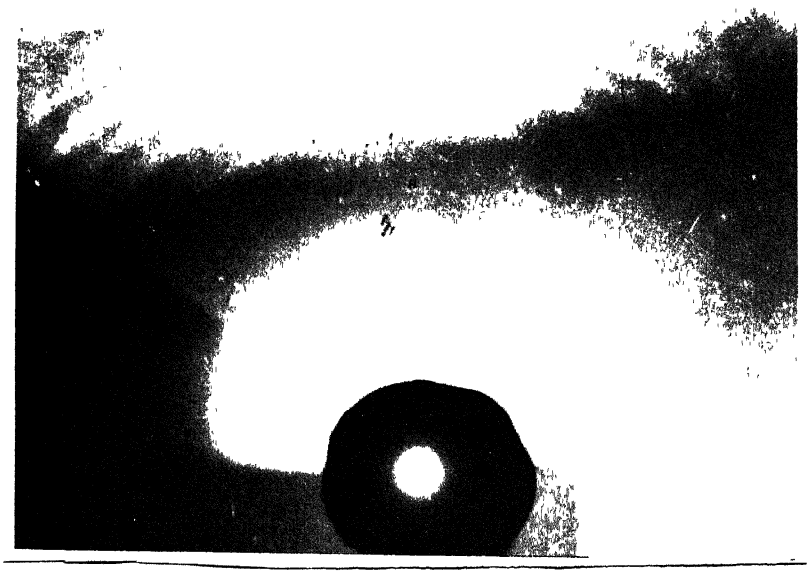

FIG 3.7 TRANSMISSION PINHOLE PATTERN OF A SUPER CONDUCTING SAMPLE EXPOSED FOR 8 HRS.

FIG. 3.8 TRANSMISSION PINHOLE PATTERN OF A SUPER CONDUCTING SAMPLE (EXPOSURE TIME IS 11 HRS.)

Table 3.3 Analysis of pinhole transmission patterns

Sample No.	Distance of spot/ ring from centre of film (R)	Bragg angle (2θ) (degrees)	Miller indices of peaks
Sample # 1 (exposure time 8 hours)	1.60	28.07	(102) or (012)
	2.00	33.69	(110)
	2.25	36.87	Y_2BaCuO_5 peak
	2.40	38.66	(005)
	2.70	41.99	(113)
	3.10	45.94	(006)
	3.35	48.15	(200)
	3.60	50.19	$BaCuO_2$ peak
Sample # 2 (exposure time 11 hours)	1.30	23.43	(003)
	2.00	33.69	(110)
	2.40	38.66	(005)
	2.70	41.99	(113)
	3.00	45.00	$Y_2Cu_2O_5$ peak
	3.30	47.33	(006)
	3.50	49.40	$BaCu_2O_5$ peak
	3.80	51.71	$Y_2Ba_2O_5$ peak
	4.70	57.45	(116)
	5.40	60.95	$Y_2Cu_2O_5$ peak

3.4 Grain Orientation:

Grain oriented samples are produced after annealing for 10 hours at 700°C. Repeated annealing treatment is found to improve grain orientations further.

Fig. 3.9 represents the x-ray diffraction patterns for different treatments. In sintered samples the strong peaks correspond to (110), (103) reflections (Fig. 3.9(a)). In Fig. 3.9(b) which corresponds to sample after an additional annealing treatment at 700°C for 10 hours in flowing Oxygen, the strongest peak correspond to (006). The other (001) type peaks are also increased.

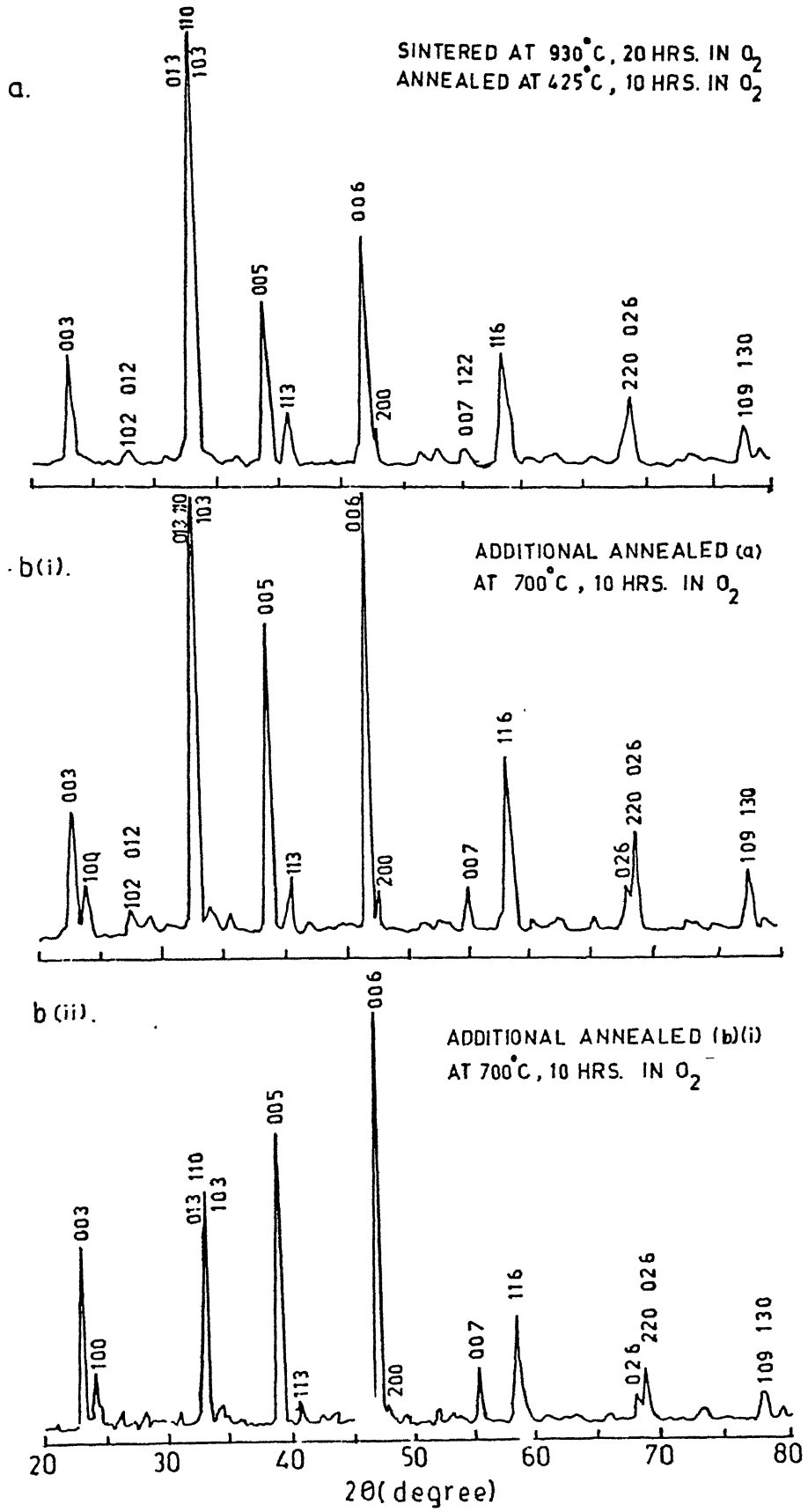

FIG. 3.9 XRD PATTERNS OF (a) AS SINTERED (b) GRAIN ORIENTED SAMPLES

By giving one more additional treatment the relative intensities of (001) peaks increased with concurrent decrease in (110), (103) peaks. This shows that grain orientations occured perpendicular to the pressure axis i.e., the c axis oriented parallel to the pressure axis with ab plane perpendicular to the pressure direction. Thus it is clear that repeated annealing treatment gives preferred orientation with c-axis parallel to the pressure direction as shown in Fig. 3.10. The preferred orientation is attributed to the grain growth. S.E.M. micrograph of the free surface of the oriented sample, annealed once, is shown in Fig. 3.11.

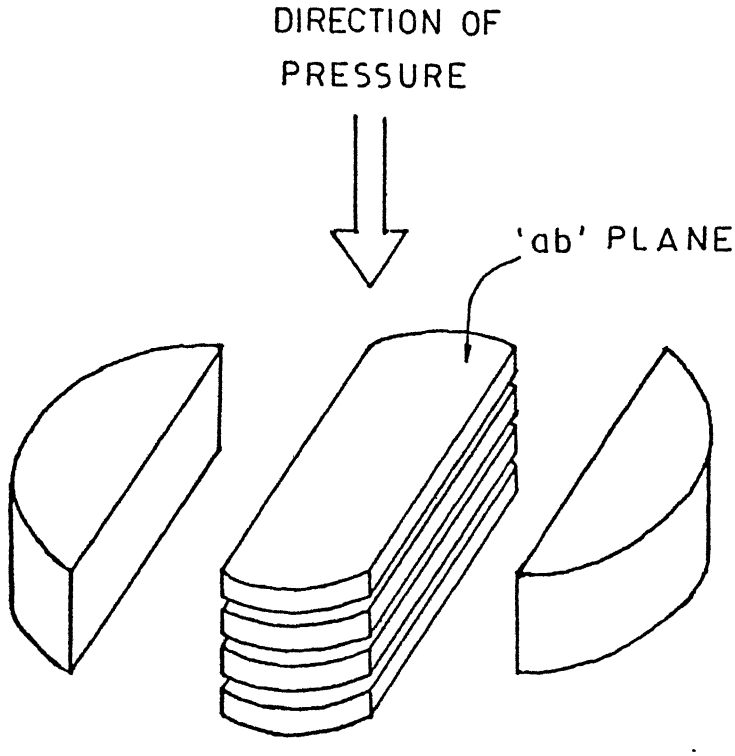

FIG. 3.10 A SCHEMATIC MODEL FOR THE REORIENTED GRAIN GROWTH

FIG. 3.11 SEM MICROGRAPH OF THE FREE SURFACE OF GRAIN ORIENTED SAMPLES (ANNEALED ONCE AT 700°C, 10HRS. IN AIR, MAGNIFIED FOUR TIMES)

CHAPTER IV

CONCLUSIONS

From the present experimental results the following conclusions can be drawn:

i) DTA studies on sintered samples indicate the presence of traces of undecomposed precursors.

ii) The XRD studies have indicated the presence of $BaCO_3$ after presintering, which is undecomposed or regenerated due to the reaction with CO/CO_2 in the ambient atmosphere. However, sintering in a flowing oxygen eliminated this problem

iii) Sintered Densities are found to increase with increasing compaction pressures upto a critical value. However, rate of heating above 800^{o}C is found to have reverse effect.

iv) X-band EPR spectrum at 9.2 GHZ modulation frequency confirmed the formation of superconducting $YBa_2Cu_3O_{7-x}$ compound. EDAX studies using SEM also confirmed this result.

v) X-ray pinhole patterns identified the presence of traces of impurity phases.

vi) Grain orientations are observed in the samples annealed at 700^{o}C, and repeated annealing improved orientation

REFERENCES

1. J.G. Bednorz and K. S. Müller, *possible High-T_c superconductivity in La-Ba-Cu-O system*, Z, Phys. B., 64(1986), p.189.

2. C.W. Chu, P.H. Hor, R.L. Meng, L. Gao, Z.J. Huang and Y.Q. Wang, *Evidence for superconductivity above 40K in the La-Ba-Cu-O compound system*,Phys. Rev. lett., 58(1987), p.405.

3. R.J. Cava, R.B. VanDover, B. Batlogg and E.A. Rietman, *Bulk superconductivity at 36K in* $La_{1.8}SrCuO_4$,Phys. Rev. Lett. 58(1987), p.408.

4. M.K. Wu, J.R. Ashburn and C.J. Torng, P.H. Hor, R.L. Meng, L. Gao, Z.J. Huang, Y.Q. Wang, and C.W. Chu, *Superconductivity at 93K in a New Mixed-phase Y-Ba-Cu-O compound system at ambient pressure*, Phys. Rev. Lett, 58(1987), p. 908.

5. R.J. Cava, B. Batlogg, R.B. VanDover, D.W. Murphy, S. Sunshine, T. Seigrist, J.P. Remeika, E.A. Rietman, S. Zahurak, and G. Espinosa, *Bulk superconductivity at 91K in single phase oxygen-deficient perovskite* $Ba_2YCu_3O_{9-\delta}$, 58(1987), p. 1676.

6. F. Izumi, H. Asano, and T. Ishigaka, *A revised structural model for the Ba-Y-Cu-O superconductor*, Jap. J. Appl. Phys., 26(1987), p.L617.

7. P.H. Hor, L. Gao, R.L. Meng, Z.J. Huang, Y.Q. Wang, K. Forster, J. Vassilious, C.W. Chu, M. K. Wu, J.R. Ashburn and C.J. Torng, *High-pressure study of the Y-Ba-Cu-O superconducting compound system*, Phys. Rev. lett. 58(1987), p. 911.

8. A.P. Molozemoff, W.J. Gallagher and R.E. Schuall, *Application of High-Temperature superconductivity*, Chemistry of High-Temperature superconductors, ed. L. Nelson, M.S. Whittingham and T.F. George, (ACS Symposium series, American Chemical Society, Washington, DC), 1987, p.280.

9. P. Murugaraj, J. Maier and A. Rabenau, *Preparation of highly oriented polycrystalline* $YBa_{2-y}Cu_3O_x$ *superconductors*, Solid State Commun., 66(1988), p.735.

10. R.R. NeurgOonkar, G. Shoop, J.R. Oliver, and I. Santha, *Hotpressed densification of high temperature superconducting* $Ba_2Ln^{3+}Cu_3O_{7-x}$ *ceramics*, Mat. Res. Bull., 23(1988), p.143.

11. Y. Nakegawa, H. Yamasaki, H. Obara, and Y. Kimura, *Superconducting properties of grain-oriented samples of* $Y_1Ba_2Cu_3O_y$, Jpn. J. Appl. Phys., 28(1929), p. L547.

12. T. Takenaka, H. Noda, A. Yoneda, and K. Sakata, *Superconducting properties of grain-oriented* $YBa_2Cu_3O_{7-x}$ *ceramics*, Jpn. J. Appl. Phys.; 27(1988), p.L209.

13. I. Weichen, X. Wu, S.J. Keating, C.Y. Keating, P.A. Johnson and T. Ying Tien, *Texture development in* $YBa_2Cu_3O_x$ *by hot extrusion and hot-pressing*, J. Am. Ceram. Soc., 70(1987).

14. G.S. Grader, H.M. O'Bryan and W.W. Rhodes, *Improved press forging of* $Ba_2YCu_3O_x$ *super conductor*, Appl. Phys. Lett., 52(1988), p. 1831.

15. S. Jin, T.H. Tiefel, R.C. Sherwood, M.E. Davis, R.B. Van Dover, G.W. kammlott, R.A. Fastnacht and H.D. Keith, *High critical currents in Y-Ba-Cu-O superconductor*, Appl. Phys. Lett., 52(1988), p. 2074.

16. Challa Ashok, N. Venkata Ramani and M.N. Shetty, *Grain-orientations in Y-Ba-Cu-O ceramic superconductors*, Jap. J. Appl. Phys. 29(1990), pp. 1097-1098.

17. Anil Khurana, *Current research*, Phys. Today, May, 1987.

18. K.G. Frase, C.G. Linger and D.R. Clarke, *Phase compatibilities in the system* Y_2O_3*-BaO-CuO at* 950^oC, J. Am. Ceram. Soc., 70(1987), p.204.

19. D.G. Hinks, L. Solderholm, D.W. Capone-II, J.D. Jorgenson, I.K. Schuller, C.V. Segre, K. Zhang and J.D. Grace, *Phase diagram and superconductivity in Y-Ba-Cu-O system*, Appl. Phys. Lett., 50(1987), p. 1688.

20. M.A. Beno, L. Solderholm, D.W. Capone-II, D.G. Hinks, J.D. Jorgenson, I.K. Schuller, C.U. Segre, K. Zhang and J.D. Grace, *Structure of the single phase high temperature superconductor* $YBa_2Cu_3O_{7-\delta}$, Appl. Phys. Lett., 51(1987), p.57.

21. M. Francois, E. Walker, J.L. Jorda, K. Yuon and P. Fischer, *Structure of the high-temperature superconductor* $Ba_2YCu_3O_7$ *by x-ray and Neutron Powder diffraction*, Solid State Commun. 63(1987), p. 1149.

22. J.E. Greedan, A.O. Reilly and C.V. Stager, *Oxygen ordering in the crystal structure of the 93K superconductor* $YBa_2Cu_3O_7$ *using powder neutron diffraction at 298 and 79.5K*, Phys. Rev. B., 35(1987), p.8770.

23. F. Izumi, H. Asano, T. Ishigaki, A. Ono and F.P. Okamura, *Crystal structure of a Ba-Y-Cu-O superconductors as revealed by reitveld analysis of x-ray powder diffraction data*, Jpn. J. Appl. Phys., 26(1987), p. 611.

24. M. Hervieu, B. domenges, C. Michel, G. hegar, J. Provost, and B. Raveau, *Twins and oriented domains in the orthorhombic superconductor* $YBa_2Cu_3O_{7-\delta}$, Phys. Rev. B., 36(1987), p. 3920.

25. C.S. Pande, A. K. Singh, L. Toth, D.U. Guber, and S. Wolf, *Domainlike defects observed in the high-temperature superconductor Y-Ba-Cu-O*, Phys. Rev. B., 36(1987), p.5669.

26. J.D. Jorgenson, M.A. Beno, D.G. Hinks, L. Soderholm, K. J. Volin, R. L. Hittterman, J.D. Grace and I.K. Schuller, *Oxygen ordering and orthorhombic to tetragonal phase transition in* $YBa_2Cu_3O_{7-x}$, Phys. Rev. B. 36(1987), p.3608.

27. A.W. Sleight, *Oxide superconductors; structure-property relationship and mechanisms for high* T_c, High tempera tue super conducting materials, ed. W.E. Hatfield and J.H. Miller, Jr., (Mercel Dekker, Newyork), 1988, p.15-23.

28. J.D. Jorgenson,*Defects and superconductivity in the copper oxides*, Physics Today, June 1991, p. 35.

29. P.K. Galagher, H.M.O'Bryan, S.A. Sunshine and D.W. Murphy, *Oxygen stoichiometry in* $Ba_2Y\ Cu_3O_x$, Mat. Res. Bull, 22(1987), p.995.

30. I. K. Schuller, D.G. Hinks, M.A. Beno, D.W. Capone II, L. Soderholm, J.P. Locquet, Y. Bruyseracde, C.U. Segre and K. Zhang, *Structural phase transition in* $YBa_2Cu_3O_{7-\delta}$; *The role of dimensionality for high-*T_c *superconductivity*, Solid State Commun., 63(1987), p. 385.

31. D.W. Murphy et. al; *Effect of Oxygen Stoichiometry on structure and properties in* $YBa_2Cu_3O_x$, Chemistry of high-T_c superconductors, ed. D.L. Welson et al. OAES Symposium Series, ACS, Washington, DC), 1987, p. 181.

32. S.P.S. Badwal et al, *Mat. Forum, 13(1989), p. 76.*

33. *J.M. Tarascon et al., High temperature oxide synthesis and chemical doping of the Cu-O planes*, Chemistry of High-T_c superconductors, ed. D. L. Nelson, M. S. Whittingham and T. P. George, (ACS Symposium Series, Washington, DC), 1987, p. 198.

34. L.E. Toth et al, *Processing of high-*T_c *ceramic superconductors; Structure and properties*, Chemistry of high-T_c superconductors, Ed. D.L. Nelson et al, (ACS Symposium series, ACS, Washington, DC), 1987, p. 228.

35. T. Kawai and M. kanai, *Preparation of Y-BA-Cu-O superconductor*, Jpn. J. Appl. Phys., 26(1987), p. L736.

36. M. Fujiki, M. Hikita and K. Sukegawa, *Preparation of a high-T_c Y-Ba-Cu-O superconductor using colloidal method*, Jpn, J. Appl. Phys., 26(1987), p. 1159.

37. K. Matsuzaki et al, *High T_c superconductor prepared by oxidation of a liquid quenched $YbBa_2Cu_3$ a;;pu fpo; om aor*, Jpn. J. Appl. Phys. 26(1987), p. L1310.

38. A.I. Kingon et al., *Processing and Microstructure of $YBa_2Cu_3O_{7-\delta}$ in high-T_c superconducting materials*, Ed. W.E. Natfield and J. H. Miller, Jr., Marcel Dekker, Inc., Newyork, 1988, p. 335.

39. H. Macde et al., *A new high T_c superconductor without a rare-earth*, Jpn, J. Appl. Phys. 27(1988) p. L209.

40. E.T. Muromachi et al, *Thermogravimetric and high temperature x-ray studies on the orthorhombic-to-tetragonal transition of $YBa_2Cu_3O_y$*, Jpn. J. Appl. Phys., 26(1987), p. L665.

41. D. larbalestier, "*Critical currents and magnete applications of High -T_c superconductors*", Phys. Today, June 1991, p. 76.

42. Challa Ashok, M.Tech. Thesis, "*Grain-Reorientations in High Temperature Ceramics*, IIT Bombay, 1990.

43. R. Jones et. al, *Synthesis, chemistry, electronic properties and magnetism in the Y-Ba-Cu-O superconductor systems in* Chemistry of high - temperature superconductors,, ed. D.L. Nelson, et al, ACS Symposium Series 351(1987), p.313.

44. W.E. Hatfield, *The advent of high temperature superconducting materials: chronology of events and Hallmark developments*, in High-Temperature Superconducting Materials, Ed. W.E. Hatfield and J. H. Miller, Jr., Marcel Dekker Inc., Newyork, 1988, p.37.

45. C.M. Srivastava and C. Srinivasan, *Superconductivity*, Science and Engineering of Materials, Wiley Eastern Ltd., (1987), p.30.

46. K.E. Easterling et al, *The processing, properties and applications of Y-Ba-Cu-O superconductors*, Materials Forum, 11(1988), p.30.

47. J. Naryan, *Microstructure and properties of High-T_c superconductors*, J. Metals, 40(1988), p.24.

48. E.T. Muramachi et al; *Thermogravimetric and high temperature x-ray studies on the Orthorhombic-to-tetragonal transition of* $YBa_2Cu_3O_y$, Jpn. J. Appl. Phys., 26(1987), p.:665.

49. E.M. Engler et al, *processing, structure and High-Temperature Superconductivity*, in Chemistry of High Temperature super conductors, Ed. D.L. Nelson, M.S. Whittingham and T.F. George, ACS Symposium serice, ACS, Washington, DC, 1987, p.265.

50. Y. Nakazawa et al, *Characterization of the High T_c superconductors* $(Ba_{0.7}Y_{0.3})CuO_{3-\delta}$, Jpn. J. Appl. Phys., 26(1987), p. L682.

51. J.Z. Sun et al., *Superconductivity and Magnetism in the High-T_c superconductor Y-Ba-Cu-O*, Phys. Rev. Lett., 58(1987), p. 266.

ME-1992-M-RAE-SOM